The EMBO Journal Vol.17 No.17 pp.4987–5000, 1998

Integrating cytosolic calcium signals into mitochondrial metabolic responses

Lawrence D.Robb-Gaspers, Paul Burnett[1], Guy A.Rutter[1], Richard M.Denton[1], Rosario Rizzuto[2] and Andrew P.Thomas[3]

Department of Pharmacology and Physiology, University of Medicine and Dentistry of New Jersey, Newark, NJ 07103, USA, [1]Department of Biochemistry, School of Medical Sciences, University Walk, University of Bristol, Bristol BS8 1TD, UK and [2]Department of Biomedical Sciences and CNR Centre for Study of Biological Membranes, University of Padova, Via Trieste 75, 35121 Padova 17, Italy

[3]Corresponding author
e-mail: thomasap@umdnj.edu

Stimulation of hepatocytes with vasopressin evokes increases in cytosolic free Ca^{2+} ($[Ca^{2+}]_c$) that are relayed into the mitochondria, where the resulting mitochondrial Ca^{2+} ($[Ca^{2+}]_m$) increase regulates intramitochondrial Ca^{2+}-sensitive targets. To understand how mitochondria integrate the $[Ca^{2+}]_c$ signals into a final metabolic response, we stimulated hepatocytes with high vasopressin doses that generate a sustained increase in $[Ca^{2+}]_c$. This elicited a synchronous, single spike of $[Ca^{2+}]_m$ and consequent NAD(P)H formation, which could be related to changes in the activity state of pyruvate dehydrogenase (PDH) measured in parallel. The vasopressin-induced $[Ca^{2+}]_m$ spike evoked a transient increase in NAD(P)H that persisted longer than the $[Ca^{2+}]_m$ increase. In contrast, PDH activity increased biphasically, with an initial rapid phase accompanying the rise in $[Ca^{2+}]_m$, followed by a sustained secondary activation phase associated with a decline in cellular ATP. The decline of NAD(P)H in the face of elevated PDH activity occurred as a result of respiratory chain activation, which was also manifest in a calcium-dependent increase in the membrane potential and pH gradient components of the proton motive force (PMF). This is the first direct demonstration that Ca^{2+}-mobilizing hormones increase the PMF in intact cells. Thus, Ca^{2+} plays an important role in signal transduction from cytosol to mitochondria, with a single $[Ca^{2+}]_m$ spike evoking a complex series of changes to activate mitochondrial oxidative metabolism.

Keywords: calcium/hepatocyte/mitochondria/proton motive force/pyruvate dehydrogenase

Introduction

Recent studies have suggested that increases in cytosolic Ca^{2+} concentration ($[Ca^{2+}]_c$) lead to parallel increases in the concentration of Ca^{2+} in mitochondria ($[Ca^{2+}]_m$), and that this is important for the stimulation of mitochondrial oxidative metabolism (McCormack *et al*., 1990; Duchen, 1992; Loew *et al*., 1994; Rizzuto *et al*., 1994; Hajnóczky *et al*., 1995; Rutter *et al*., 1996b). In particular, it has been proposed (Rizzuto *et al*., 1993) that there is preferential targeting to mitochondria of Ca^{2+} released from endoplasmic reticulum (ER) stores as a result of the positioning of mitochondrial Ca^{2+} uptake channels close to ER release sites. Similar results in a number of cell types (Hajnóczky *et al*., 1995; Rutter *et al*., 1996b) have supported this hypothesis. In addition to the transmission of cytosolic Ca^{2+} signals to the mitochondria, it is also apparent that mitochondrial Ca^{2+} uptake can modulate $[Ca^{2+}]_c$ dynamics (Nicholls, 1978; Jouaville *et al*., 1995; Budd and Nicholls, 1996; Simpson and Russell, 1996; Babcock *et al*., 1997; Hoth *et al*., 1997).

One set of targets regulated by the $[Ca^{2+}]_m$ increases elicited in response to Ca^{2+}-mobilizing hormones are the intramitochondrial dehydrogenases, pyruvate dehydrogenase (PDH), NAD^+-isocitrate dehydrogenase (NAD^+-ICDH) and 2-oxoglutarate dehydrogenase (OGDH). Whereas Ca^{2+} ions interact directly with NAD^+-ICDH and OGDH to decrease the K_m values for substrates (Denton *et al*., 1978; McCormack and Denton, 1979; Rutter, 1990), the effects of Ca^{2+} on PDH involve an increase in the active, dephosphorylated form of the enzyme, mediated by a Ca^{2+}-sensitive phosphatase (Denton *et al*., 1972, 1996). These findings have led to a model in which the mitochondrial NAD(P)H redox couple is regulated directly by $[Ca^{2+}]_m$ linked to $[Ca^{2+}]_c$ changes (Denton and McCormack, 1980; McCormack *et al*., 1990; Hansford, 1994). However, each of the dehydrogenases is also sensitive to regulation by metabolites. For example, phosphorylation of the PDH complex is catalyzed by a specific PDH kinase, which is activated by increasing the ratios of ATP/ADP, NADH/NAD^+ or acetyl CoA/CoA (Reed and Yeaman, 1987). Similarly, increases in ATP/ADP and NADH/NAD^+ ratios directly inhibit NAD^+-ICDH and OGDH (Denton *et al*., 1978; McCormack and Denton, 1979; Rutter, 1990).

In earlier studies, we demonstrated in fibroblasts a clear correlation between changes in $[Ca^{2+}]_m$ and the level of active PDH (Rutter *et al*., 1996b). However, studies in single living hepatocytes (Pralong *et al*., 1994; Hajnóczky *et al*., 1995) have suggested that the relationship between $[Ca^{2+}]_m$ and intramitochondrial NAD(P)H is more complex. For example, we found that the close coupling between $[Ca^{2+}]_m$ and oxidative metabolism assessed through changes in NAD(P)H fluorescence was lost after the initial rapid $[Ca^{2+}]_m$-dependent phase of NADP(H) reduction (Hajnóczky *et al*., 1995). As a result, sustained redox responses were initiated by transient changes in $[Ca^{2+}]_c$ (spiking). Paradoxically, the redox responses were not sustained at high agonist doses that caused a sustained elevation in $[Ca^{2+}]_c$. This divergence between $[Ca^{2+}]_c$ signals and activation of mitochondrial metabolism occurs

© Oxford University Press

at the level of mitochondrial Ca^{2+} uptake and not Ca^{2+}-dependent stimulation of intramitochondrial dehydrogenases. We proposed that efficient and rapid Ca^{2+} uptake into the mitochondria occurs only during active Ca^{2+} mobilization from internal stores, which corresponds to the rising phase of the $[Ca^{2+}]_c$ oscillation (Hajnóczky *et al*., 1995). Thus, high agonist doses that generate a sustained increase in $[Ca^{2+}]_c$ elevate $[Ca^{2+}]_m$ only transiently. The activation of Ca^{2+}-sensitive intramitochondrial dehydrogenases would be predicted to follow the changes in $[Ca^{2+}]_m$ (Hajnóczky *et al*., 1995). However, the NAD(P)H reoxidation rate is slow relative to the decline in $[Ca^{2+}]_m$ (Hajnóczky *et al*., 1995). This suggested that intramitochondrial metabolism is regulated by hormones through additional mechanisms, or the activity state of the Ca^{2+}-sensitive dehydrogenases declines more slowly than $[Ca^{2+}]_m$. For example, the slow fall in NADP(H) could be due to a slow rephosphorylation and consequent inactivation of PDH.

The present study was undertaken with two principal aims: (i) to investigate the relationship between $[Ca^{2+}]_m$ and PDH during a single $[Ca^{2+}]_m$ spike; and (ii) to analyze the relationship between PDH activation and NAD(P)H changes. Therefore, the level of the active, dephosphorylated form of PDH (PDH_a) has been measured synchronously with pyridine nucleotide redox state following stimulation with a high dose of vasopressin. This hormone, which elicits Ca^{2+} release through the generation of inositol 1,4,5-trisphosphate (IP_3), has been shown previously to activate PDH in suspensions of liver cells and in the perfused liver (Hems *et al*., 1978; Oviasu and Whitton, 1984). However, the effects of the hormone on PDH_a have not been examined in the attached primary cultures of hepatocytes used to study $[Ca^{2+}]_c$, $[Ca^{2+}]_m$ and NADP(H) responses in single cells. By using Ca^{2+}-sensitive fluorescent dyes localized to the mitochondria in single-cell measurements, and recombinant targeted aequorins in cell populations, we demonstrate that high doses of vasopressin provoke a sustained rise in $[Ca^{2+}]_c$, but a transient increase in $[Ca^{2+}]_m$. Analysis of the kinetics of the subsequent changes in PDH_a, NAD(P)H and mitochondrial proton motive force (PMF) suggest that Ca^{2+}-dependent changes in PDH are only one of a number of factors controlling mitochondrial redox changes after a single $[Ca^{2+}]_m$ spike. Our data indicate that hepatic mitochondria convert a single $[Ca^{2+}]_m$ spike into prolonged PDH stimulation, followed by increased respiratory chain activity. Interplay between Ca^{2+}-dependent activation and metabolic feedback regulation of PDH, the citric acid cycle dehydrogenases and the respiratory chain gives rise to the complex pattern of NAD(P)H changes following agonist stimulation.

Results

Relationship between $[Ca^{2+}]_c$, $[Ca^{2+}]_m$ and PDH activity in vasopressin-stimulated hepatocytes

In previous studies of hormone-induced $[Ca^{2+}]_c$ oscillations, we demonstrated that each individual $[Ca^{2+}]_c$ 'spike' elicited a transient increase in NAD(P)H fluorescence, and that the resulting NAD(P)H oscillations merged to give a sustained elevation of NAD(P)H at high $[Ca^{2+}]_c$ oscillation frequencies (Hajnóczky *et al*., 1995). In order to elucidate the metabolic events underlying these Ca^{2+}-induced changes in mitochondrial NAD(P)H levels in the present study, it was necessary to establish conditions where changes in $[Ca^{2+}]_c$ and $[Ca^{2+}]_m$ occurred synchronously throughout a population of cells. Since submaximal vasopressin concentrations yield asynchronous oscillations in these parameters, we chose a maximal dose of vasopressin that gave a synchronous increase in $[Ca^{2+}]_c$, which was then sustained in the entire cell population. Hepatocytes incubated for the PDH assay were cultured in an identical manner, but on polylysine-coated Petri dishes. No differences were observed in the response of $[Ca^{2+}]_c$ or $[Ca^{2+}]_m$ to vasopressin challenge for cells plated on polylysine-coated glass or plastic (not shown).

As reported previously (Hajnóczky *et al*., 1995), 50 nM vasopressin evoked a sustained increase in $[Ca^{2+}]_c$, measured with cytosolic fura-2, accompanied by a transient, synchronized increase in $[Ca^{2+}]_m$, measured with the mitochondrial rhod-2 (Figure 1A). Stimulation of rhod-2-loaded hepatocytes with vasopressin evoked increases in $[Ca^{2+}]_m$ that could also be detected within single mitochondria, co-localized with the membrane potential-insensitive dye, Mito Tracker Green (MTG) (Figure 2A). The increase in $[Ca^{2+}]_m$ reported by rhod-2 fluorescence had similar kinetics in all of the mitochondria within a single cell, but the relative amplitude was significantly larger in peripheral mitochondria. The mechanism for the larger $[Ca^{2+}]_m$ increase in peripheral mitochondria is unknown, although it should be noted that the overall density of mitochondria is lower in the cell periphery. The average rhod-2 fluorescence intensity from all mitochondria increased 229 $\pm$ 35% after vasopressin stimulation ($>$150 mitochondrial measurements/cell; $n = 4$).

In order to obtain a calibrated measure of $[Ca^{2+}]_m$ and to confirm that the increase in $[Ca^{2+}]_m$ was indeed transient, we expressed the recombinant Ca^{2+}-sensitive photoprotein, aequorin, targeted to mitochondria via the signal sequence of subunit VIII of cytochrome *c* oxidase (Rizzuto *et al*., 1992; Rutter *et al*., 1996a,b). Immunocytochemical analysis of the distribution of the hemagglutinin (HA) epitope tag of the aequorin construct revealed characteristic and exclusive mitochondrial staining, either in a single optical slice (Figure 2D) or after superimposition of multiple slices (Figure 2E). Stimulation of mitochondrial aequorin-expressing hepatocytes with 50 nM vasopressin yielded a transient increase in light output, which could be calibrated (Rutter *et al*., 1993) to reveal a peak increase of $[Ca^{2+}]_m$ to 1.96 $\pm$ 0.22 μM, with a time-to-peak of 13.6 $\pm$ 4.0 s ($n = 7$ separate hepatocyte preparations). $[Ca^{2+}]_m$ then recovered to near-resting values ($<$200 nM) within 2 min. These data confirmed that stimulation of the cells with 50 nM vasopressin produced a single, transient spike in $[Ca^{2+}]_m$.

A rapid increase in cellular NAD(P)H fluorescence, which predominantly reflects changes in the mitochondrial NADH in the hepatocytes and perfused liver (Avi-Dor *et al*., 1962; Sugano *et al*., 1980; Hajnóczky *et al*., 1995), occurred synchronously with the increase in $[Ca^{2+}]_m$, but decayed more slowly (Figure 1B). We have speculated that this could reflect the activation and deactivation of the PDH complex (Hajnóczky *et al*., 1995). We therefore tested this hypothesis directly in synchronized cell populations. As expected, a rapid initial phase of PDH activation

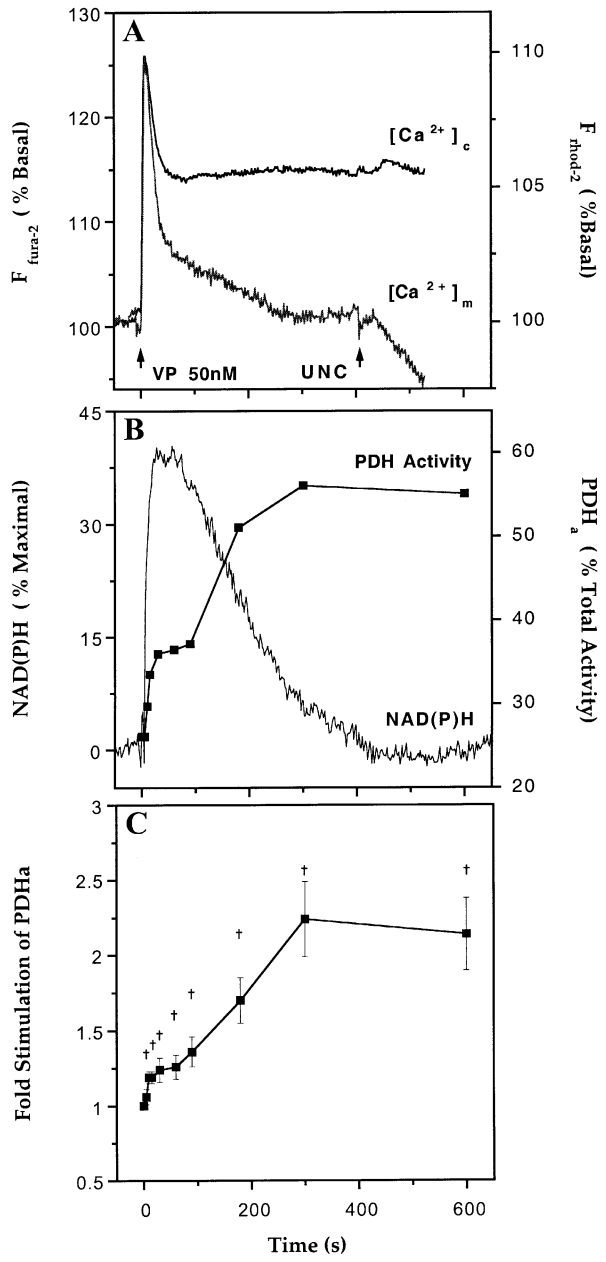

Fig. 1. Relationship between vasopressin-induced Ca^{2+}-mobilization and intramitochondrial metabolism. In (A–C), 50 nM vasopressin (VP) was present continuously from time zero [first arrow shown in (A)]. (**A**) Simultaneous measurement of mean $[Ca^{2+}]_c$ and $[Ca^{2+}]_m$ responses in primary cultured rat hepatocytes co-loaded with fura-2 and rhod-2. To improve temporal resolution, fura-2 fluorescence changes were monitored at 380 nm only. Mitochondrial localization of rhod-2 fluorescence signals was confirmed by the addition of the mitochondrial uncoupler, 1799 (5 μg/ml) plus oligomycin (5 μg/ml), (UNC). (**B**) Effect of maximal vasopressin on mitochondrial NAD(P)H and PDH_a activity. NAD(P)H responses were monitored using 360 nm autofluorescence in unloaded hepatocytes. The mean fluorescence signal calculated from all cells in the imaging field was normalized to the peak 360 nm fluorescence intensity obtained after the addition of rotenone (5 μg/ml) plus 10 mM β-hydroxybutyrate (see Figures 5 and 6). Mean PDH_a activity was measured in triplicate from the same hepatocyte preparation at the indicated time points. PDH_a activity is expressed as a percentage of the maximal PDH activity present in the extract. (**C**) Mean PDH_a activity from four different hepatocyte preparations measured in triplicate. The data are expressed as a percentage of PDH_a activity prior to vasopressin stimulation. The symbol, † designates PDH_a values significantly different from that at time zero ($P \leqslant 0.05$).

followed stimulation with vasopressin, and was correlated with the NAD(P)H rise, achieving a transient plateau after 30 s. This behavior of the PDH complex is consistent with the rapid transfer of Ca^{2+} from ER Ca^{2+} stores into mitochondria, as previously proposed (Rizzuto *et al*., 1993, 1994; Hajnóczky *et al*., 1995; Rutter *et al*., 1996b). However, whereas NAD(P)H fluorescence began to decline to basal levels 60–100 s after stimulation (Figure 1B), a second phase of PDH activation then ensued (Figure 1B and C). This observation raises two questions: (i) since $[Ca^{2+}]_m$ has declined essentially to basal levels 2 min after stimulation, what mechanism is responsible for the further increase in PDH_a; and (ii) why should NAD(P)H levels begin to fall in the face of increased PDH_a? To investigate question (i), we determined whether other, metabolic factors were responsible for the changes in PDH activity.

$[Ca^{2+}]_m$-independent mechanisms of PDH activation

In addition to the regulation of PDH phosphate phosphatase by Ca^{2+}, the phosphorylation state of the PDH complex is regulated by several cofactors that modulate the activity of PDH kinase (Reed and Yeaman, 1987; Denton *et al*., 1996). We first tested the possibility that a decrease in acetyl CoA:CoA ratio, which would inactivate PDH kinase and therefore increase PDH_a, could occur during the second phase of PDH activation (Figure 1B and C). Inhibition of fatty acid oxidation by vasopressin might be expected to result in a decrease in the ratio of acetyl CoA:CoA. We tested this hypothesis by stimulating hepatocytes with vasopressin in the presence of a concentration of D-carnitine sufficient to block the transport of long chain fatty acids across the inner mitochondrial membrane (Figure 3). The presence of D-carnitine caused an unexpected small decrease in basal PDH_a prior to vasopressin challenge, but the extent and kinetics of the subsequent vasopressin-induced activation were unaffected (Figure 3). Incubation with L-carnitine to enhance the oxidation of fatty acyl-CoA and increase acetyl-CoA caused the excepted decrease in basal PDH_a. However, like D-carnitine, L-carnitine was without effect on the subsequent vasopressin-induced activation of PDH (Figure 3). These findings eliminated changes in fatty acid oxidation as a likely cause of the second phase of PDH activation following vasopressin stimulation.

We next tested the role of ATP:ADP changes in altering the level of PDH_a; a fall in this ratio would be predicted to activate the complex by inhibition of PDH kinase activity. As shown in Figure 4A and B, vasopressin stimulation evoked a rapid and sustained decrease in cellular ATP of ~15%. Similar behavior has been observed recently in HeLa cells stimulated with another IP_3-generating agonist, histamine (L.S.Jouaville, C.Bastianutto and R.Rizzuto, unpublished data). Furthermore, vasopressin potentiated the decrease in ATP resulting from treatment with the mitochondrial ATP synthase inhibitor, oligomycin (Figure 4B). However, vasopressin stimulation did not potentiate the fall in cellular ATP in the presence of the mitochondrial ATP translocase inhibitor, atractyloside. The kinetics of the vasopressin-induced decrease in the ATP:ADP ratio suggest that this may act in concert with an increase in $[Ca^{2+}]_m$ to achieve the first phase of PDH

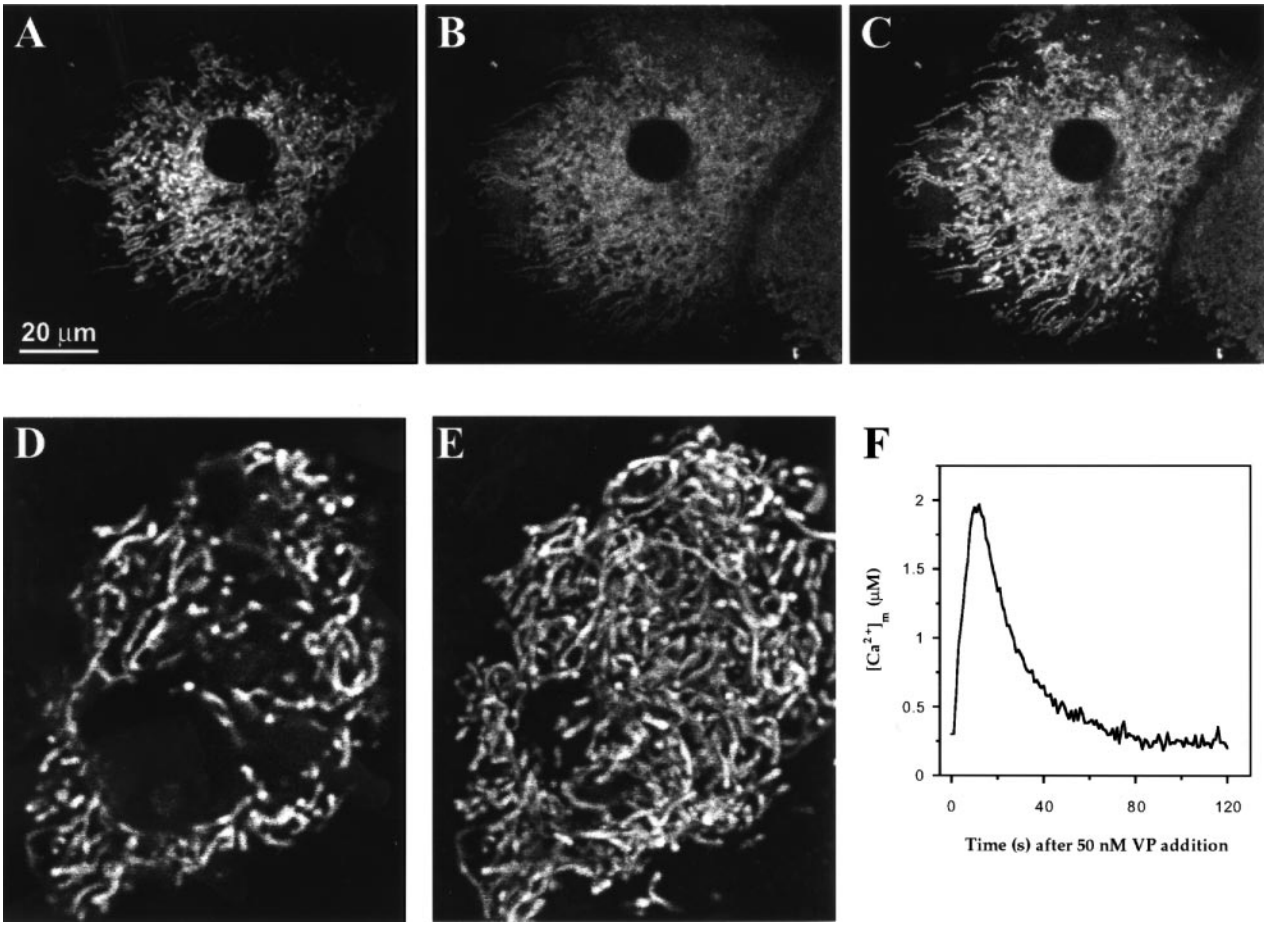

Fig. 2. Subcellular localization of rhod-2 fluorescence changes during vasopressin (VP) stimulation (A–C) and calibration of the Ca^{2+} changes as $[Ca^{2+}]_m$ using mitochondrial-targeted aequorin (D–F). Dual wavelength confocal microscopy was used to obtain simultaneous images of Mito Tracker Green (**A**), to visualize mitochondrial morphology, and Ca^{2+}-sensitive rhod-2 (**B** and **C**) to monitor $[Ca^{2+}]_m$ changes in a single hepatocyte. Rhod-2 fluorescence images were obtained before (B) and 30 s after addition of 50 nM vasopressin (C). (**D** and **E**) Primary cultured hepatocytes transiently transfected with the plasmid pCMV*Aq_m containing the HA epitope tag and mitochondrial-targeted aequorin. At 24 h post-transfection, paraformaldehyde-fixed hepatocytes were stained for the HA tag as described in Materials and methods. (D) is a single confocal section through a hepatocyte and (E) is the reconstructed image from a series of confocal sections. (**F**) Calculated $[Ca^{2+}]_m$ changes from a population of primary cultured hepatocytes transfected with mitochondrial-targeted aequorin. The trace has been aligned to the 50 nM vasopressin addition at time zero.

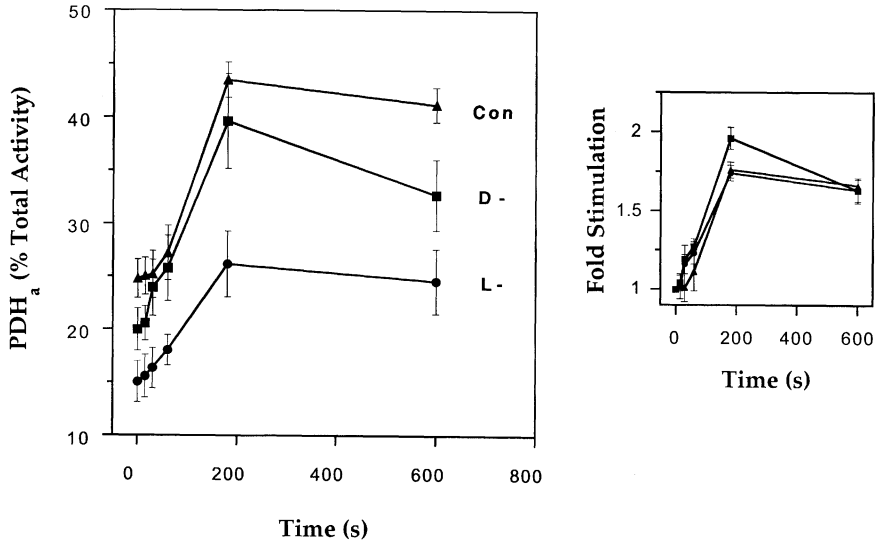

Fig. 3. Effect of inhibiting mitochondrial fatty acid transport on the magnitude and kinetics of the vasopressin-induced rise in PDH_a. Hepatocytes were plated on poly-D-lysine-coated Petri dishes and maintained in primary culture for 90 min. The cells were then washed and pre-incubated for 40–60 min either in KR-HEPES buffer (Con; ▲) or in KR-HEPES buffer supplemented with 2 mM D-carnitine (D-; ■) or L-carnitine (L-; ●). Hepatocytes were stimulated with 50 nM vasopressin at time zero and PDH_a activity assayed at the indicated time points. PDH_a was measured in triplicate from two hepatocyte preparations. Insert: PDH_a normalized to the basal levels of PDH_a for each condition.

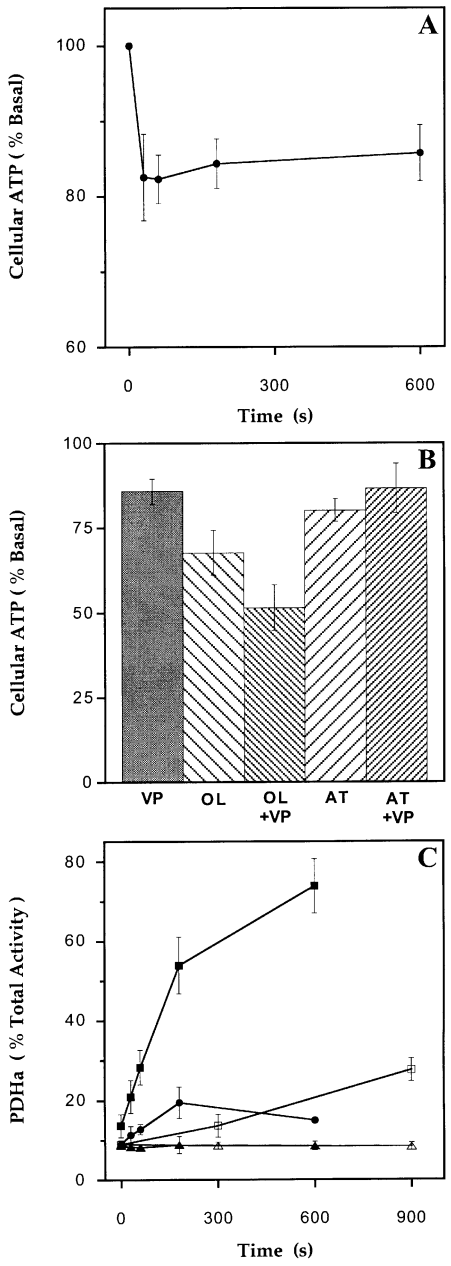

Fig. 4. Relationship between cellular ATP levels and PDH_a in primary cultured hepatocytes. Hepatocytes were plated and cultured for 90 min on poly-D-lysine-coated Petri dishes, then washed and pre-incubated for 40–60 min in KR-HEPES buffer prior to the addition of agonist or inhibitor. (**A**) Effect of 50 nM vasopressin (VP) on cellular ATP levels. Hepatocytes were stimulated with 50 nM vasopressin at time zero and ATP levels determined at the indicated time points. ATP was assayed in triplicate from four different hepatocyte preparations and normalized to total cellular protein measured in a parallel culture from the same cell preparation. Basal ATP levels were 9.0 ± 2.6 nmol/mg protein. (**B**) Effect of oligomycin and atractyloside on cellular ATP levels in the presence or absence of 50 nM vasopressin. Hepatocytes were treated for 10 min with either: 50 nM vasopressin (VP); 5 μg/ml oligomycin (OL); vasopressin plus oligomycin (OL + VP); 5 μg/ml atractyloside (AT); or vasopressin plus atractyloside (AT + VP). (**C**) Effect of mitochondrial ATP synthase and ATP translocase blockers on basal and vasopressin-stimulated PDH_a activity. Cultured hepatocytes were incubated in the presence of 50 nM vasopressin (●), 5 μg/ml oligomycin (□), vasopressin plus oligomycin 5 μg/ml (■), atractyloside (△) or vasopressin plus atractyloside (▲). PDH_a was determined in triplicate at the indicated times (data from two hepatocyte preparations).

activation (Figure 1B and C). However, it is unlikely that the decrease in cellular ATP content could entirely explain the second phase of PDH activation (beginning ~2 min after vasopressin exposure) since, during this time, a new steady-state level of ATP had been achieved. Nevertheless, the slow component of PDH activation closely paralleled the reoxidation of NAD(P)H (Figure 1B). Therefore, the decline in NAD(P)H, which would tend to decrease the activity of PDH kinase, may gradually unmask the effect of the rapid decline in ATP. Thus, the second phase of PDH activation can be explained by a sustained fall in mitochondrial ATP, combined with the time-dependent fall in NAD(P)H.

To test further the hypothesis that the sustained changes in the level of PDH_a after a vasopressin challenge could be mediated by alterations in intramitochondrial ATP, we examined the effect of oligomycin and atractyloside on vasopressin stimulation of PDH (Figure 4C). Oligomycin pre-incubation would be expected to decrease mitochondrial [ATP], whereas the presence of atractyloside should maintain a high $[ATP]_m$. Inhibition of mitochondrial ATP synthesis dramatically potentiated the effects of vasopressin challenge on the increase in PDH_a (Figure 4C). In contrast, blockade of mitochondrial ATP:ADP transport with atractyloside entirely prevented the vasopressin-induced increase in PDH_a (Figure 4C). Strikingly, the potentiation by vasopressin of the oligomycin-induced increase in PDH_a, and the absence of any effect of vasopressin on PDH_a in the presence of atractyloside (Figure 4C), matched the effects of vasopressin on ATP levels in the presence of each inhibitor (Figure 4B). These data suggest that the second phase of PDH activation can be explained by the combined effect of an increase in cytosolic ATP consumption in the presence of the hormone, resulting in a fall in $[ATP]_m$ and a subsequent reoxidation of NAD(P)H.

Role of PDH in the control of mitochondrial NAD(P)H levels after vasopressin stimulation

The fact that NAD(P)H fell in the face of an increase in PDH_a during the latter period of vasopressin stimulation (Figure 1B) suggested that alterations in PDH activity may not be the primary determinant of NAD(P)H levels. In order to test this hypothesis directly, we examined the response of mitochondrial NAD(P)H to a large increase in the level of PDH_a using the specific PDH kinase inhibitor, dichloroacetate (DCA; Whitehouse *et al*., 1974). DCA has no effect on the citric acid cycle dehydrogenases, NAD^+-ICDH and OGDH. Exposure of hepatocytes to 2 mM DCA for 5 min caused an increase in the proportion of PDH_a to 55 ± 2.0% of total activity compared with a control value of 21.0 ± 0.5% (n = 3 separate preparations). Nevertheless, DCA addition caused a partial oxidation of NAD(P)H in the absence of agonist (Figure 5). Moreover, subsequent challenge with 50 nM vasopressin prompted an increase in PDH_a to 97.0 ± 6.0% (assayed 60 s after stimulation), and a similar rate and extent of NAD(P) reduction was observed in the presence and absence of DCA (Figure 5). Although pre-activation of PDH with DCA did not grossly perturb the NADP(H) response to vasopressin, DCA pre-treatment resulted in a small decrease in the magnitude of pyridine nucleotide reduction (6.2 ± 1.5%; n >100 cells from two cell preparations;

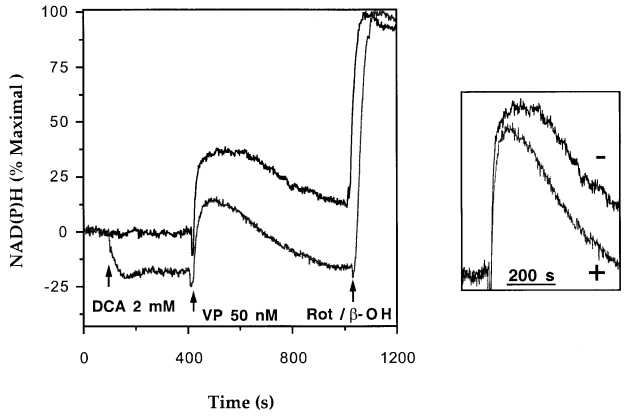

Fig. 5. Effect of dichloroacetic acid (DCA) on the vasopressin-induced increase in NAD(P)H. Primary cultured hepatocytes were stimulated with 50 nM vasopressin (VP) in the presence (lower trace) or absence (upper trace) of 2 mM DCA, an inhibitor of PDH kinase. NAD(P)H responses were monitored using 360 nm excitation, and normalized to the fluorescence intensity obtained after addition of rotenone (5 μg/ml) plus 10 mM β-hydroxybutyrate (Rot/β-OH). Each trace represents the mean fluorescence response of all cells in the imaging field. Insert: vasopressin-induced increases in NAD(P)H replotted with the baselines adjusted to account for the direct effect of DCA prior to vasopressin addition. The + symbol denotes the presence of DCA. See the text for details of PDH_a levels in these experiments.

Figure 5, inset) and an earlier onset of the NAD(P)H reoxidation phase when compared with untreated hepatocytes. These data indicate that the vasopressin-induced increase in PDH_a is only one of the mechanisms by which the redox state of the mitochondrial NAD(P)H couple is modified. Furthermore, since the secondary phase of PDH activation is expected to increase NAD(P)H production at a time when NAD(P)H reoxidation is occurring, it is clear that alternative mechanisms of regulation must predominate during this phase.

Mechanisms of NAD(P)H reoxidation

The results described above led us to search for further mechanisms that might be responsible for the late phase decline in NAD(P)H. One possible mechanism is activation of the mitochondrial respiratory chain after hormone stimulation, resulting in an enhanced rate of NAD(P)H oxidation. A transient increase in cellular NAD(P)H fluorescence accompanied by a sustained stimulation of the mitochondrial respiratory rate has been observed in isolated hepatocyte suspensions challenged with a high vasopressin dose (Balaban and Blum, 1982; Quinlan and Halestrap, 1986; Halestrap, 1989; Brown *et al*., 1990). Brown *et al*. (1990) have also shown that β-hydroxybutyrate increases both NAD(P)H and mitochondrial respiratory rate, but not to the same extent as observed during vasopressin stimulation. Evidence that vasopressin increases the rate of NAD(P)H oxidation in cultured hepatocytes was provided by the observation that addition of β-hydroxybutyrate to naive cells caused a sustained increase in NAD(P)H (Figure 6A), whereas addition of β-hydroxybutyrate to cells pre-treated with vasopressin caused only a transient increase (Figure 6B). The gradual reoxidation of NAD(P)H in the presence of hormone could be explained by a time-dependent increase in respiratory chain activity. When vasopressin was added after β-hydroxybutyrate, the hormone still caused a large increase in NAD(P)H and a significantly faster rate of NAD(P)H reoxidation compared with β-hydroxybutyrate alone (Figure 6C). The enhanced rate of NAD(P)H reoxidation could be explained by the ability of Ca^{2+}-mobilizing hormones to stimulate mitochondrial respiratory chain flux (Quinlan and Halestrap, 1986; Brown *et al*., 1990; reviewed in Hoek, 1992). NAD(P)H reoxidation could not be accounted for by Ca^{2+}-dependent activation of the malate–aspartate shuttle (Strzelecki *et al*., 1988; Sugano *et al*., 1988), which transfers reducing equivalents into the cytosol, because NAD(P)H reoxidation was unaffected by the transaminase inhibitor aminooxyacetate (Figure 6D).

Further evidence that increased respiratory chain activity was responsible for the reoxidation of NAD(P)H comes from the data shown in Figure 7. Addition of oligomycin to inhibit mitochondrial ATP synthetase, and hence decrease flux through the respiratory chain, caused a substantial increase in the extent of mitochondrial pyridine nucleotide reduction (Figure 7A). Subsequent treatment with vasopressin caused a further, sustained increase in redox state in the oligomycin-treated cells. The sustained nature of the NAD(P)H increase suggests that vasopressin does not stimulate its reoxidation when respiratory chain activity is limited by preventing ATP synthesis. However, the lack of NAD(P)H reoxidation could also be explained by activation of the other Ca^{2+}-sensitive dehydrogenases (NAD^+-ICDH and OGDH), which are stimulated allosterically by a fall in intramitochondrial ATP:ADP ratio. Therefore, we used the mitochondrial adenine nucleotide translocase inhibitor atractyloside to inhibit respiratory chain flux whilst maintaining high intramitochondrial ATP:ADP. This agent had no effect on mitochondrial NAD(P)H in the absence of vasopressin but, in common with oligomycin, it converted the transient increase in NAD(P)H usually observed with vasopressin to a sustained response (Figure 7B). Under these conditions, control of respiratory chain flux is shifted to the adenine nucleotide translocase, such that respiratory chain activation by vasopressin would not be reflected in enhanced NAD(P)H reoxidation. Figure 7 shows that oligomycin and atractyloside had no effect on basal $[Ca^{2+}]_c$ or the $[Ca^{2+}]_c$ response to vasopressin measured simultaneously with NAD(P)H fluorescence. Moreover, these inhibitors did not prevent the vasopressin-induced $[Ca^{2+}]_m$ transient measured with aequorin (Figure 7).

Vasopressin-induced elevation of mitochondrial PMF

Stimulation of respiratory chain activity independent of energy utilization is expected to result in an increase in the PMF across the inner mitochondrial membrane. The PMF is composed of membrane potential ($\Delta\Psi_m$) and pH gradient (ΔpH_m) components. Although it has not been shown for vasopressin, a number of previous studies have suggested that gluconeogenic hormones such as glucagon, α-adrenergic agonists and L-triiodothyronine increase the PMF in hepatocyte suspensions and perfused liver (Prpic *et al*., 1978; Taylor *et al*., 1980; Soboll and Scholz, 1986; Halestrap, 1989; Soboll *et al*., 1992; Soboll, 1993). However, the measurements of PMF in these studies were carried out in mitochondrial fractions isolated from the cells or tissue subsequent to hormone treatment. In the

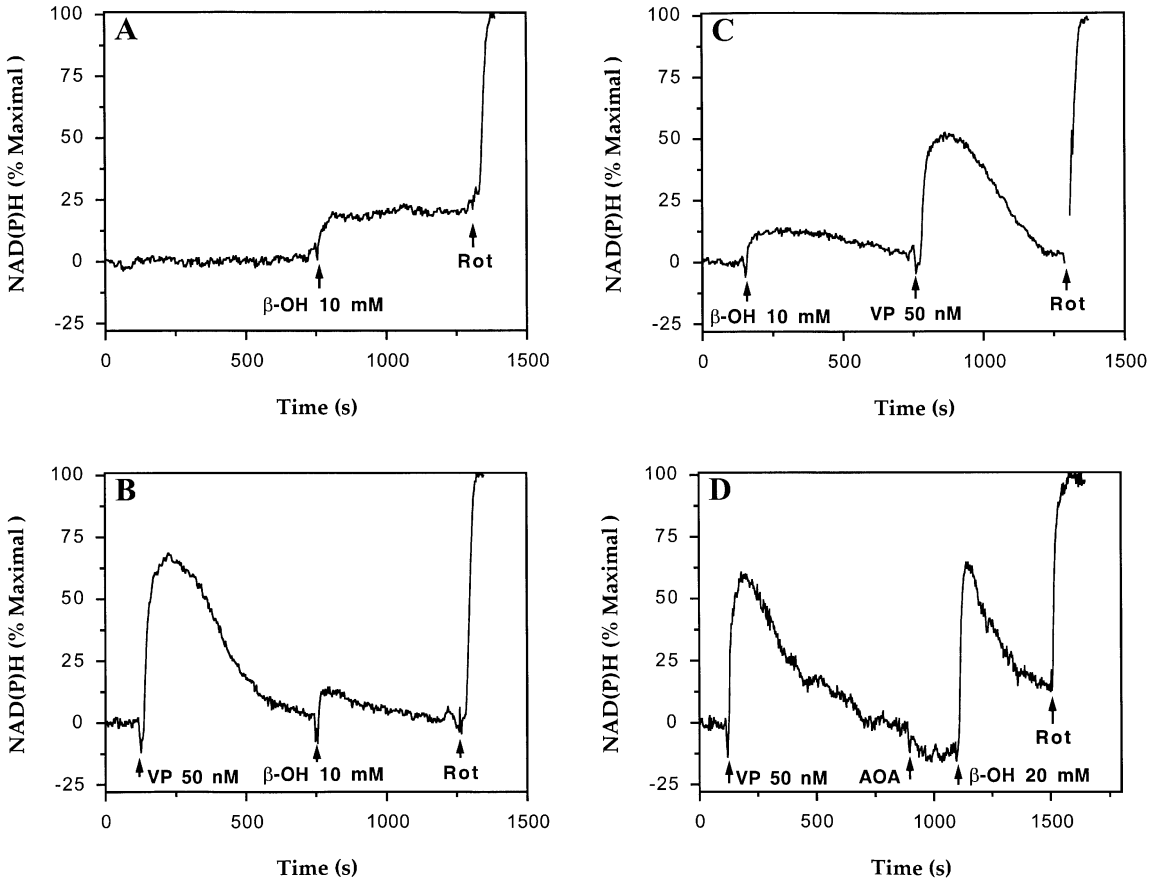

Fig. 6. NAD(P)H reoxidation rate in control and vasopressin-stimulated hepatocytes. β-Hydroxybutyrate (β-OH) was added to primary cultured hepatocytes either alone (**A**), after (**B**) or before (**C**) the addition of 50 nM vasopressin (VP). In (**D**), 2 mM aminooxyacetate (AOA), an inhibitor of the malate–aspartate shuttle, was added prior to the addition of β-OH. NAD(P)H responses were monitored using 360 nm excitation, and normalized to the fluorescence intensity obtained after the addition of rotenone (5 μg/ml; Rot). Each trace represents the mean NAD(P)H response of all cells in the imaging field (50–100 cells), and is representative of three or more similar experiments.

present work, we have used fluorescent indicators to monitor changes in $\Delta\Psi_m$ and ΔpH_m of intact living cells in real-time during stimulation with vasopressin. The cultured hepatocytes were incubated with the weak acid fluorescein, which distributes across the mitochondrial inner membrane according to ΔpH_m, or with the potential-sensitive dye, tetramethylrhodamine ethyl ester (TMREE) (Thomas *et al*., 1991; Loew *et al*., 1993). Vasopressin stimulation of single hepatocytes caused a significant and time-dependent increase in both mean fluorescein and TMREE fluorescence intensities, indicating a relative increase in ΔpH_m and $\Delta\Psi_m$ (Figure 8A and B). The rates of rise of ΔpH_m and $\Delta\Psi_m$ after vasopressin stimulation were much slower than the $[Ca^{2+}]_c$ and $[Ca^{2+}]_m$ responses, but more closely paralleled the reoxidation of NAD(P)H and the second phase of PDH activation. Increases in mitochondrial PMF were more sustained than the changes in NAD(P)H, but returned towards basal values after prolonged stimulation (Figure 8B). Vasopressin-induced changes in PMF do not appear to result from increased supply of reducing equivalents to the respiratory chain, since addition of β-hydroxybutyrate prior to the stimulus had little effect on ΔpH_m (Figure 8A). In addition, aceto-acetate treatment to shift the mitochondrial NAD(P)H redox couple to a more oxidized state caused only a slight depression of the vasopressin-induced increase in ΔpH_m (Figure 8A). Addition of β-hydroxybutyrate elevated $\Delta\Psi_m$, but did not alter changes in $\Delta\Psi_m$ in response to vasopressin (not shown).

A key question is whether the vasopressin-induced changes in mitochondrial PMF are mediated through a Ca^{2+}-dependent mechanism. Therefore, hepatocytes were pre-loaded with BAPTA-AM (40 μM) to block vasopressin-stimulated $[Ca^{2+}]_c$ responses, allowing us to monitor for Ca^{2+}-independent effects of the agonist on mitochondrial PMF. The BAPTA loading protocol was only effective in 10–20% of hepatocytes, yielding either completely blocked (Figure 9A) or truncated $[Ca^{2+}]_c$ responses (compare Figures 8B and 9B) to supramaximal vasopressin stimulation. For the remaining cells, BAPTA pre-loading did not significantly affect the mean $[Ca^{2+}]_c$ or mean $\Delta\Psi_m$ responses to high vasopressin stimulation, presumably because the loading was less efficient (data not shown). In cells where BAPTA pre-loading blocked the $[Ca^{2+}]_c$ response to vasopressin stimulation, the agonist-dependent increase in $\Delta\Psi_m$ was also inhibited (Figure 9A). Vasopressin treatment did gradually increase $\Delta\Psi_m$ in cells where BAPTA pre-loading only blunted the $[Ca^{2+}]_c$ response (Figure 9B). However, in these cells, the rate of rise in $\Delta\Psi_m$ after vasopressin treatment was slow when compared with cells not loaded with BAPTA (Figure 8B) or when BAPTA loading had no effect on vasopressin-

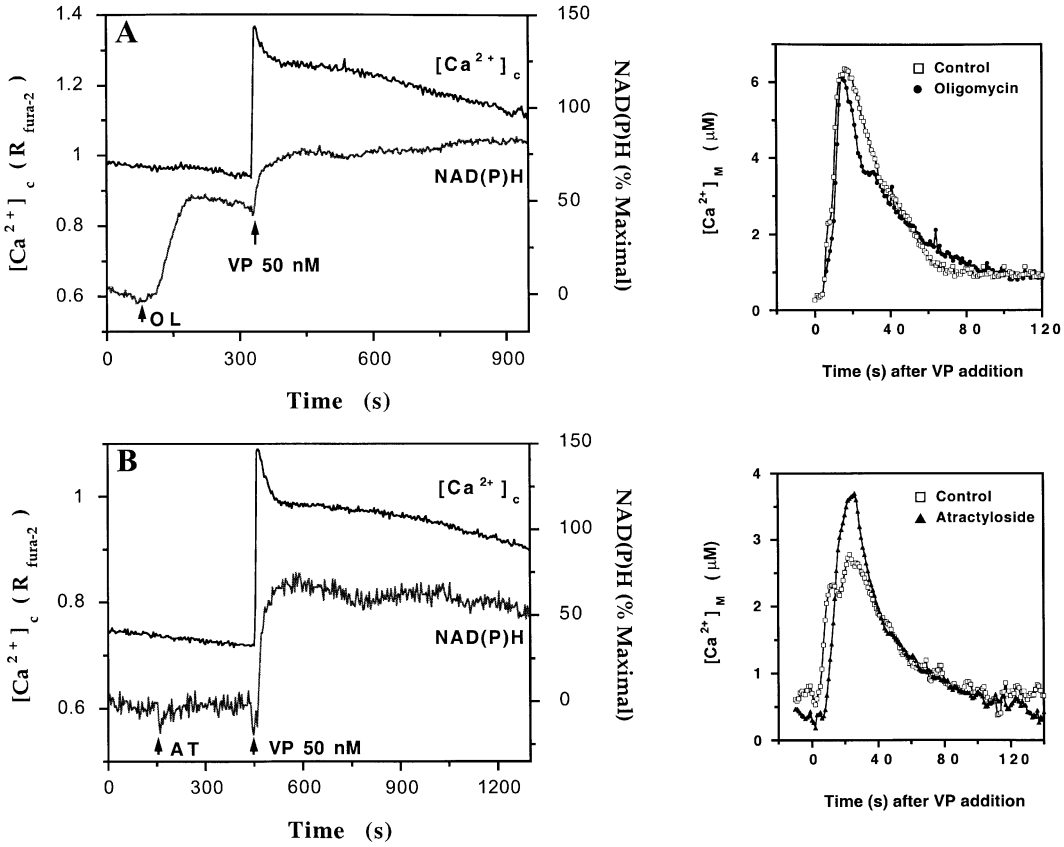

Fig. 7. Effect of oligomycin and atractyloside on the reoxidation of NAD(P)H and changes in $[Ca^{2+}]_m$ following vasopressin (VP) addition. Simultaneous measurements of $[Ca^{2+}]_c$ and NAD(P)H were carried out in primary cultured hepatocytes loaded with a low level of fura-2. In (**A**), the ATP/ADP ratio was reduced by addition of the mitochondrial ATP synthetase inhibitor oligomycin (5 μg/ml; OL), whereas in (**B**) a high intramitochondrial ATP/ADP ratio was achieved by inhibition of the adenine nucleotide translocase with atractyloside (5 μg/ml; AT). Hepatocytes were pre-incubated with the inhibitors for 5 min prior to the addition of 50 nM vasopressin. Mean NAD(P)H responses were normalized to the fluorescence intensity obtained after the addition of rotenone (5 μg/ml) plus 10 mM β-hydroxybutyrate (not shown), and are representative of two or more experiments. Insert: the effects of oligomycin and atractyloside on vasopressin-induced increases in $[Ca^{2+}]_m$ measured in cultured hepatocytes transfected with mitochondrial-targeted aequorin.

induced $[Ca^{2+}]_c$ responses (not shown). The data of Figure 9A and B clearly illustrate that an elevation of $[Ca^{2+}]_c$ is a prerequisite for the vasopressin-evoked increase in $\Delta\Psi_m$.

Further evidence that the increase in mitochondrial PMF is mediated through a Ca^{2+}-dependent mechanism is shown in Figure 9C and D. In these experiments, $[Ca^{2+}]_c$ was increased in the absence of receptor activation by the addition of thapsigargin. We have shown previously that treatment of hepatocytes with thapsigargin elevates both $[Ca^{2+}]_c$ and $[Ca^{2+}]_m$, although the increase in $[Ca^{2+}]_m$ is delayed relative to the $[Ca^{2+}]_c$ response (Hajnóczky *et al.*, 1995). Figure 9C shows the mean $[Ca^{2+}]_c$ and mean ΔpH_m responses, and Figure 9D shows the mean $[Ca^{2+}]_c$ and mean $\Delta\Psi_m$ responses after the addition of thapsigargin. Cellular responses were measured simultaneously in fura-2- and fluorescein-loaded hepatocytes or in fura-2- and TMREE-loaded hepatocytes, respectively. Thapsigargin treatment caused an immediate, slow rise in $[Ca^{2+}]_c$, which remained elevated for the duration of the experiment (Figure 9C and D). Thapsigargin addition also stimulated a robust increase in both fluorescein and TMREE fluorescence, indicating a relative increase in total mitochondrial PMF (Figure 9C and D). In fluorescein- and fura-2-co-loaded hepatocytes, there was a consistent delay of 30–60 s between thapsigargin-induced $[Ca^{2+}]_c$ increases and the initiation of the increase in ΔpH_m (Figure 9C). This delay in the ΔpH_m response is similar to what we previously reported for thapsigargin-evoked changes in both NAD(P)H and $[Ca^{2+}]_m$ (Hajnóczky *et al.*, 1995). However, we did not observe such a clear-cut delay in the thapsigargin-evoked increase in $\Delta\Psi_m$ (Figure 9D). While we have not yet identified the site(s) at which calcium exerts its effect on PMF, the data shown in Figure 9 clearly demonstrate that increases in mitochondrial PMF are mediated through a Ca^{2+}-dependent pathway. These data represent the first direct evidence that the total PMF is increased in intact cells after treatment with vasopressin.

In order to obtain a quantitative estimate of the changes in PMF, fluorescein fluorescence was expressed as a ratio to the minimal fluorescence values obtained after addition of uncoupler (1799) plus oligomycin at the end of each experiment. This fluorescence ratio is related directly to ΔpH_m (Thomas *et al.*, 1991). TMREE fluorescence changes were normalized to the maximum and minimum fluorescence intensities obtained after addition of nigericin to hyperpolarize the mitochondrial inner membrane, followed by 1799 plus oligomycin to collapse the PMF (Figure 8B). Vasopressin stimulation induced an increase in TMREE fluorescence equal to 10 ± 0.6% (n >100 cells from two

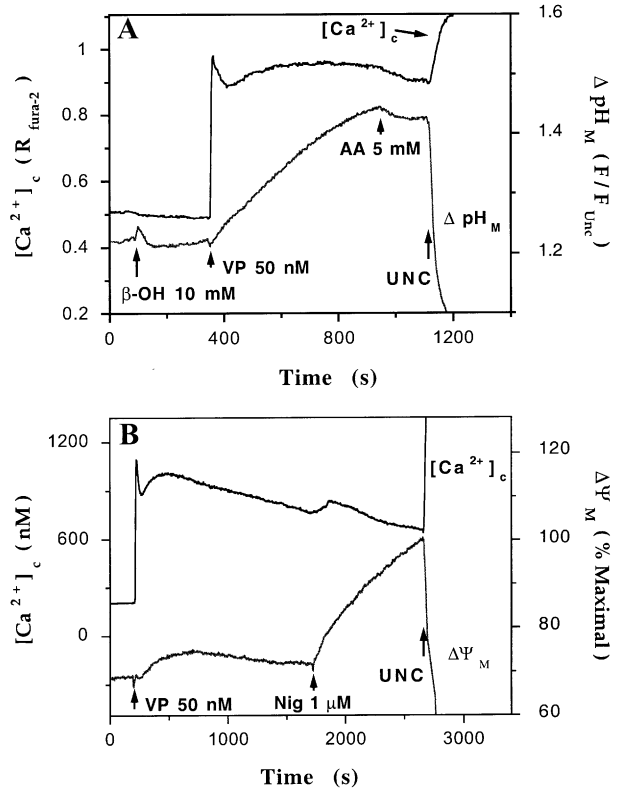

Fig. 8. Relationship between $[Ca^{2+}]_c$ and mitochondrial PMF. (**A**) Simultaneous measurements of $[Ca^{2+}]_c$ and ΔpH_m in cultured hepatocytes stimulated with 50 nM vasopressin (VP). $[Ca^{2+}]_c$ was measured using fura-2 while ΔpH_m was monitored with fluorescein. Fluorescein fluorescence was normalized to the values obtained after the addition of the uncoupler 1799 (5 μg/ml) plus oligomycin (5 μg/ml) (UNC). This fluorescence ratio reports the relative changes in the ΔpH_m (Thomas *et al*., 1991). Addition of β-OH followed by acetoacetate (AA) to reduce and then oxidize mitochondrial NADH did not significantly affect the magnitude of the changes in ΔpH_m. (**B**) Simultaneous measurements of $[Ca^{2+}]_c$ and $\Delta\Psi_m$ in cultured hepatocytes stimulated with 50 nM vasopressin. $[Ca^{2+}]_c$ was measured using fura-2 and $\Delta\Psi_m$ was monitored with TMREE. The TMREE fluorescence traces were normalized to a maximal range of $\Delta\Psi_m$ by first hyperpolarizing the mitochondrial inner membrane using the K^+/H^+ ionophore nigericin (Nig), followed by collapse of $\Delta\Psi_m$ with the uncoupler 1799 (5 μg/ml) plus oligomycin (5 μg/ml) (UNC). The TMREE fluorescence intensities are expressed as a percentage of the fluorescence intensity difference between these two conditions. All traces represent the mean of changes observed in all cells in the imaging field.

preparations) of the full range from uncoupler-depolarized to the maximal polarization with nigericin. Utilizing confocal microscopy and very low levels of laser excitation, the changes in ΔpH_m and $\Delta\Psi_m$ could also be observed at the level of individual mitochondria (Figure 10A and B, see also Figure 2E). From confocal images similar to that shown in Figure 10A, the apparent ΔpH_m can be calculated from the log of the ratio of the mitochondrial to cytosolic fluorescein fluorescence intensities, assuming a linear relationship between fluorescence and indicator concentration. Basal ΔpH_m was estimated to be 0.29 ± 0.01 pH units ($n = 4$ cells, >600 mitochondria) and 0.43 ± 0.01 pH units ($n = 5$ cells, >1200 mitochondria) after vasopressin stimulation. This analysis probably underestimates the magnitude of ΔpH_m, since the optical section used to acquire the confocal images probably extends to some degree beyond the volume expected to be occupied by the mitochondrial matrix space (see Loew *et al*., 1993). The limitations of using confocal microscopy to determine dye distribution across a single mitochondrion were even more evident when $\Delta\Psi_m$ was calculated from the mitochondrial to cytosolic TMREE fluorescence ratio. For the cell shown in Figure 10B, the mean basal TMREE fluorescence ratio was 79, and this increased to 151 in the presence of vasopressin (n >700 mitochondria). This converts into a $\Delta\Psi_m$ of –114 mV under basal conditions and –130 mV after vasopressin stimulation. Basal $\Delta\Psi_m$ has been reported previously to be –160 mV in isolated hepatocyte suspensions and –145 mV in the intact perfused liver (Hoek *et al*., 1980; Soboll *et al*., 1992; Soboll, 1993), suggesting that the resolution limitations in the confocal imaging approach may underestimate the absolute value of $\Delta\Psi_m$. Nevertheless, these data clearly demonstrate that vasopressin increases both the $\Delta\Psi_m$ and ΔpH_m components of the PMF in individual hepatocytes, and give an estimate of ~20% for the magnitude of total PMF increase.

Discussion

The current study was undertaken to elucidate the mechanisms responsible for the complex pattern of mitochondrial redox changes in response to intracellular $[Ca^{2+}]$ increases following vasopressin treatment of hepatocytes. We have used a mode of stimulation in which a simultaneous and sustained increase in $[Ca^{2+}]_c$ and a single transient spike of $[Ca^{2+}]_m$ occur in all the cells within a population of hepatocytes. This has allowed us to monitor the time course and extent of the subsequent downstream mitochondrial events. The ionic and metabolic changes occurring in the mitochondria after stimulation with a high concentration of vasopressin fall into three phases (Figures 1, 4 and 8). During the first phase, from 0 to 25 s (phase I), there is a rapid increase in $[Ca^{2+}]_m$, followed after a 2–3 s lag by an increase in NAD(P)H (Figure 1A and B). This presumably reflects the Ca^{2+}-dependent activation of PDH (Figure 1B and C) and the citric acid cycle dehydrogenases, NAD^+-ICDH and OGDH. During phase I, there is also a decrease in cellular ATP levels, which remain depressed from ~30 s after stimulation (Figure 4A). During the next phase (phase II, 25–60 s after stimulation), $[Ca^{2+}]_m$ returns to basal levels (Figures 1A and 2F). PDH_a and NAD(P)H levels remain relatively stable during this phase. In phase III (60 s and later), NAD(P)H levels decay back to basal by ~400 s after vasopressin addition (Figure 1B), while PDH_a increases to a stable plateau over a similar time frame (Figure 1B and C). Increases in ΔpH_m and $\Delta\Psi_m$ are initiated after the peak $[Ca^{2+}]_c$ rise and continue through phase III, reaching a peak value ~600 s after the start of the $[Ca^{2+}]_c$ response (Figures 8 and 10). Both ΔpH_m and $\Delta\Psi_m$ gradually return to baseline values during prolonged stimulation.

The data presented here provide a number of important insights into the mechanism of Ca^{2+} signaling from cytosol to mitochondria, and how these signals are translated into the ultimate metabolic responses of the cell. We have used both fluorescent Ca^{2+} indicators and targeted aequorins to confirm that $[Ca^{2+}]_m$ increases only transiently, even in the face of a sustained increase of $[Ca^{2+}]_c$ evoked by maximal vasopressin. This dissociation of Ca^{2+} signals between the two compartments presumably reflects the

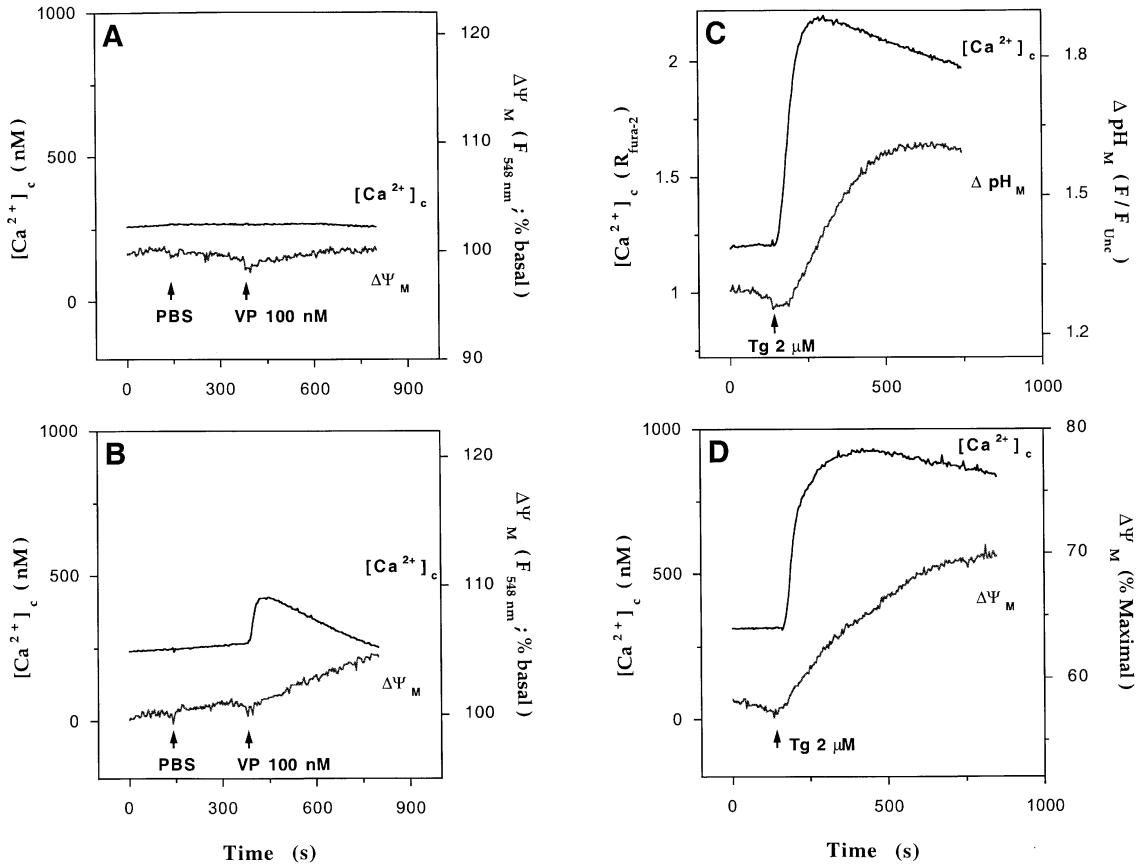

Fig. 9. Role of Ca^{2+} in the vasopressin (VP)-induced increases in mitochondrial PMF. (**A** and **B**) Primary cultured hepatocytes were co-loaded with BAPTA-AM (40 μM) plus fura-2 AM (5 μM) for 40 min prior to loading with TMREE. $[Ca^{2+}]_c$, and $\Delta\Psi_m$ responses were measured simultaneously as described in the legend to Figure 8. The addition of buffer control (PBS, 30 μl) and vasopressin are indicated by the arrows. Traces are the mean cellular responses for nine (A) and 11 (B) cells from the same experiment. TMREE fluorescence changes are expressed as a percentage of basal. (**C**) Simultaneous measurements of $[Ca^{2+}]_c$ and ΔpH_m in cultured hepatocytes treated with 2 μM thapsigargin (Tg). Fluorescein fluorescence was normalized to the values obtained after the addition of FCCP (5 μM) plus oligomycin (5 μg/ml) (not shown). (**D**) Simultaneous measurements of $[Ca^{2+}]_c$ and $\Delta\Psi_m$ in cultured hepatocytes treated with 2 μM Tg. The TMREE fluorescence traces were normalized to a maximal range of $\Delta\Psi_m$ by first hyperpolarizing the mitochondrial inner membrane with nigericin (2 μM), followed by collapsing $\Delta\Psi_m$ with FCCP (5 μM) plus oligomycin (5 μg/ml) (not shown). The TMREE fluorescence intensities are expressed as a percentage of the fluorescent intensity difference between these two conditions. In (C) and (D), traces represent the mean cellular responses observed in all cells in the imaging field (50–100 cells). Similar results were obtain in three different hepatocyte preparations.

privileged availability of Ca^{2+} released from the ER for uptake by the mitochondria (Rizzuto *et al.*, 1993, 1994; Hajnóczky *et al.*, 1995; Rutter *et al.*, 1996b), which only occurs during the initial rapid phase of ER Ca^{2+} release. The local $[Ca^{2+}]_c$ gradients underlying this privileged transfer of Ca^{2+} to the mitochondria do not persist when the ER Ca^{2+} stores are depleted at high levels of vasopressin (Hajnóczky *et al.*, 1995). The initial spike of $[Ca^{2+}]_m$ is sufficient to activate mitochondrial Ca^{2+}-sensitive dehydrogenases, including an increase in PDH_a, to generate a rapid rise in NAD(P)H. Nevertheless, the phosphorylation state of the PDH complex is clearly not the only determinant of the redox state of mitochondrial pyridine nucleotides. For example, manipulation of PDH_a with DCA had rather limited effects on the pattern of NAD(P)H changes in response to vasopressin (Figure 5). Furthermore, the time dependences of the changes in NAD(P)H and PDH_a following hormone stimulation were only linked in the early phase of the response (phase I; Figure 1). Therefore, increases in $[Ca^{2+}]_m$ correlate only with this initial phase of PDH activation. Subsequently, PDH_a continued to rise despite the decline of $[Ca^{2+}]_m$ to basal levels (phases II and III). The secondary increase in PDH_a is largely attributable to changes in the levels of two intramitochondrial metabolites, ATP and NADH, which are also regulators of the dehydrogenases that are allosterically regulated by $[Ca^{2+}]_m$ (NAD^+-ICDH and OGDH). The decrease in cellular ATP is likely to be due to the activation by vasopressin of cytosolic ATP-requiring processes (e.g. gluconeogenesis, Ca^{2+} extrusion).

Despite the large and persistent activation of PDH by vasopressin, we observed that the increase in NAD(P)H levels was not sustained, but declined during phase III of the response. The fall in ATP levels could contribute to the decline in NAD(P)H, because a lower ATP:ADP ratio is expected to enhance flux through the respiratory chain. However, the changes in [ATP] occurred more rapidly than the decline of NAD(P)H (compare Figures 1 and 4). Moreover, if the respiratory chain was stimulated by the lower level of ATP, this should have been accompanied by a fall in PMF. Instead, we observed an increase in both the $\Delta\Psi_m$ and ΔpH_m components of the PMF. Taken together with the declining NAD(P)H level, the increase in PMF indicates that vasopressin treatment led to a direct

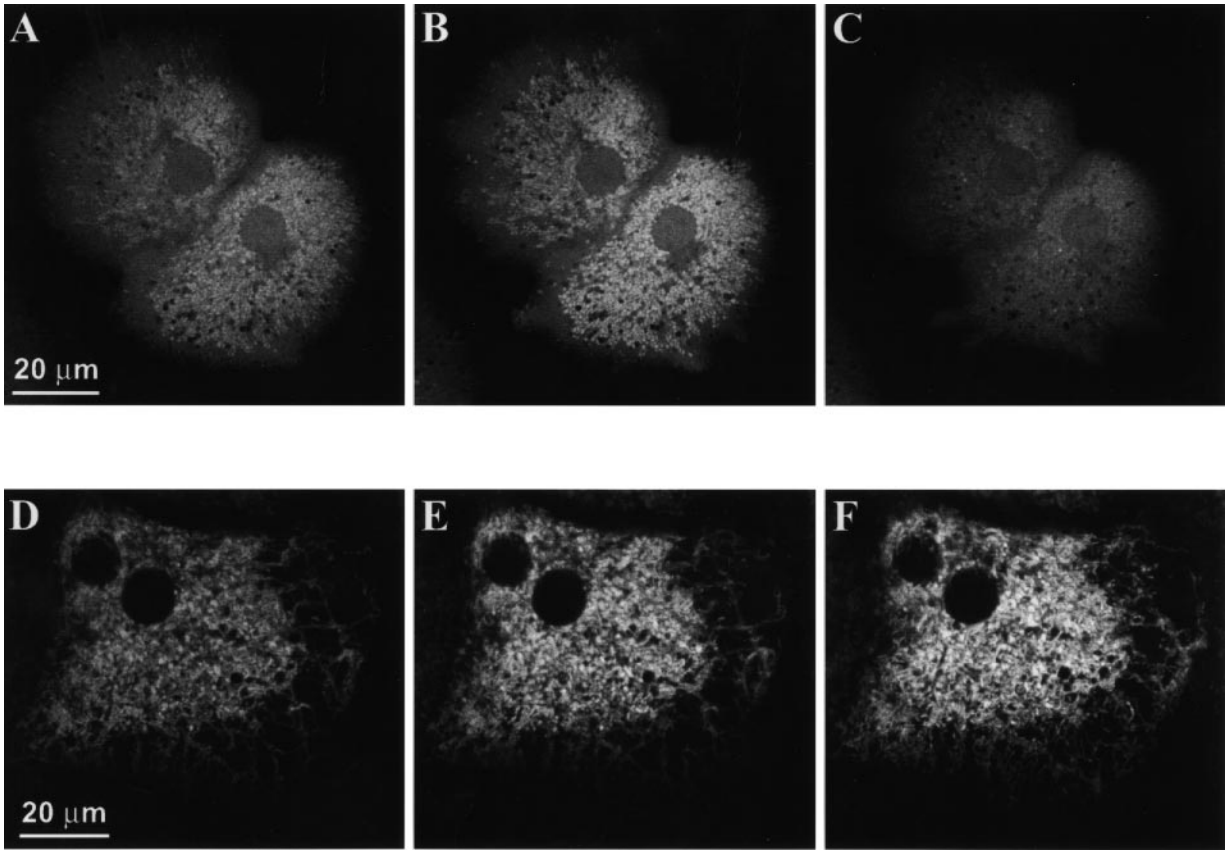

Fig. 10. Subcellular organization of ΔpH_m and $\Delta\Psi_m$ changes induced by vasopressin in individual hepatocytes. (A–C) Each panel depicts a confocal image of fluorescein fluorescence shown in a linear gray scale. Confocal images were acquired before (**A**) and 5 min after (**B**) the addition of 50 nM vasopressin. Mitochondrial localization was confirmed by the addition of the uncoupler, 1799 (5 μg/ml) plus oligomycin (5 μg/ml) (**C**). (D–F) Confocal images of TMREE fluorescence depicted in a linear gray scale. Images were acquired before (**D**) and 5 min after the addition of 50 nM vasopressin (**E**). (**F**) The maximal fluorescence intensity changes obtained 15 min after the addition of the K^+/H^+ ionophore nigericin (1 μM).

stimulation of respiratory chain activity. While we cannot at this stage identify the site(s) at which Ca^{2+} acts, our data indicate that Ca^{2+} mobilization is absolutely required for vasopressin to augment the PMF (Figure 9). Furthermore, thapsigargin can also elevate the PMF, strengthening the concept that Ca^{2+} ions mediate the increase in PMF (Figure 9). There have been a number of previous studies demonstrating increased respiratory chain activity or increases in PMF components in isolated mitochondria obtained from animals or cells treated with hormones such as glucagon, vasopressin and triiodothyronine. However, the present work represents the first direct demonstration of a hormone-induced increase in PMF measured in intact cells. Moreover, our ability to make these measurements at the single cell level has allowed us to define how the changes in PMF relate to the $[Ca^{2+}]_c$ and $[Ca^{2+}]_m$ signals generated by vasopressin treatment. The PMF components return to baseline values slowly after high vasopressin stimulation, even though the increase in $[Ca^{2+}]_m$ is more transient. It should also be noted that the increased mitochondrial PMF should have important effects on mitochondrial Ca^{2+} uptake during oscillatory $[Ca^{2+}]_c$ signaling, since the initial rate of Ca^{2+} uptake in hepatic mitochondria is proportional to the magnitude of the $\Delta\Psi_m$ (Gunter *et al.*, 1994). This suggests that not only can $[Ca^{2+}]_c$ signals regulate mitochondrial function but, once activated, the mitochondria are poised to modify subsequent incoming Ca^{2+} signals. Thus, the progressive enhancement of mitochondrial Ca^{2+} uptake could act to reduce the $[Ca^{2+}]_c$ in the vicinity of the mitochondria.

A number of previous studies have used cell suspensions and isolated mitochondria to investigate the mechanism by which Ca^{2+}-dependent hormones activate the respiratory chain. Halestrap and co-workers have obtained evidence that respiratory chain activation occurs at the level of electron flow into the ubiquinone pool (Halestrap and Dunlop, 1986; Quinlan and Halestrap, 1986; Halestrap, 1989). These workers suggested that this results from an increase in mitochondrial volume, which is mediated by a $[Ca^{2+}]_m$-dependent accumulation of inorganic pyrophosphate (Davidson and Halestrap, 1987; Halestrap, 1989). However, our studies indicate that respiratory chain activation continues despite the return of $[Ca^{2+}]_m$ to basal levels. This apparent hysteresis could reflect the time required for the accumulation of pyrophosphate to trigger a mitochondrial volume increase. It is also possible that the transient increase in $[Ca^{2+}]_m$ generates another, long lasting intramitochondrial signal to activate the respiratory chain. Alternatively, respiratory chain activity may be partially regulated by $[Ca^{2+}]_c$ levels.

In summary, changes in NAD(P)H levels following vasopressin stimulation and the accompanying single spike in $[Ca^{2+}]_m$ result from a complex interplay between several processes. These include the early activation of the mitochondrial dehydrogenases by Ca^{2+}, followed later by increases in respiratory chain activity. Our data provide

a molecular explanation for the dynamic changes in PDH_a following vasopressin stimulation, involving a transient increase in $[Ca^{2+}]_m$ and subsequent alterations in ATP and NADH levels that further activate the enzyme. Similarly, the reoxidation of the NAD(P)H couple occurring in phase III of the response to vasopressin can be attributed to the activation of the respiratory chain, manifest as an increase in both the $\Delta\Psi_m$ and ΔpH_m components of the PMF. Thus, the integrated metabolic response to Ca^{2+}-dependent hormones includes stimulation of both the supply of respiratory substrates and flux through the respiratory chain, concomitant with the increase in metabolic energy demand for anabolic pathways such as gluconeogenesis. In addition to its role in signal transduction from cell surface receptors to the cytoplasm, Ca^{2+} also functions in the transduction of signals from the cytosol to the mitochondria to allow concerted regulation of cellular metabolism.

Materials and methods

Hepatocyte isolation and culture

Hepatocytes were isolated by a two-step collagenase perfusion of livers from fed male Sprague–Dawley rats essentially as described by Rooney *et al*. (1989), with the following modifications. Rat livers were perfused with the collagenase-containing buffer until fissures formed underneath the liver capsule when subjected to gentle pressure. The liver was minced, resuspended in the collagenase buffer supplemented with 1 mM $CaCl_2$ and incubated for an additional 5 min in a shaking water bath. Hepatocytes were washed, then plated on poly-D-lysine (5 $\mu g/cm^3$)-coated glass coverslips or 35 mm plastic Petri dishes and maintained in primary culture for 1.5–3 h in Williams' E medium (WEM) plus 10% fetal calf serum (FCS) as described by Hajnóczky *et al*. (1995). Hepatocytes used in confocal imaging experiments were cultured overnight in WEM supplemented with insulin. Prior to use, the cells were washed then pre-incubated for 40–60 min in KR-HEPES buffer composed of (in mM): 121 NaCl, 25 Na-HEPES, 5 $NaHCO_3$, 4.7 KCl, 1.2 KH_2PO_4, 1.2 $MgSO_4$, 2.0 $CaCl_2$, 10 glucose, 3 L-lactate, 0.3 pyruvate and 0.25% (w/v) essentially fatty acid-free bovine serum albumin (BSA; Sigma fraction V), pH 7.4 at 37°C. When stated in the text, 2 mM D-carnitine or 2 mM L-carnitine were also present during the pre-incubation period.

Imaging measurements of $[Ca^{2+}]_c$, $[Ca^{2+}]_m$ and NAD(P)H

$[Ca^{2+}]_c$ was measured using fura-2 essentially as described previously (Rooney *et al*., 1989; Hajnóczky *et al*., 1995). Briefly, primary cultured hepatocytes on glass coverslips were loaded with 5 μM fura-2 AM (TEFLABS, Austin, TX) for 20–30 min in the presence of 100 μM bromosulfophthalein (BSP) and 0.01% (w/v) pluronic acid F-127. BSP, a competitive anion transport inhibitor, was included to inhibit loss of the Ca^{2+} indicator dye. BSP did not affect viability or inhibit $[Ca^{2+}]_c$ responses. When $[Ca^{2+}]_c$ was measured alone, fura-2-loaded hepatocytes were washed twice with KR-HEPES without dye or pluronic acid and transferred to a thermostatically regulated microscope chamber (37°C). Fluorescence images were acquired with a cooled charge-coupled device (CCD) camera under computer control and alternating excitation at 340 and 380 nm, as described previously (Rooney *et al*., 1989; Hajnóczky *et al*., 1995). Simultaneous measurement of $[Ca^{2+}]_c$ and NAD(P)H was performed in hepatocytes loaded with low levels of fura-2 AM, as described by Hajnóczky *et al*. (1995), except that BSP was used instead of sulfinpyrazone. The 360 nm fluorescence intensity or NAD(P)H signal was corrected for spillover from the Ca^{2+}-free form of fura-2 and photobleaching. Fura-2 fluorescence spillover was corrected by subtracting a fraction of the 380 nm fluorescence intensity signal from the 360 nm signal (Chiavaroli *et al*., 1994). The correction factor was determined from the ratio of the fluorescence decrease in the 360 nm signal to the fluorescence decrease in the 380 nm signal during an increase in $[Ca^{2+}]_c$. A separate correction factor was determined for each individual experiment. Photobleaching rate was corrected for by fitting a single exponential to the baseline 360 nm fluorescence signal. The best fit exponential equation was used to construct a separate trace that described the photobleaching rate over the time course of the experiment. This trace was then added to the 360 nm fluorescence intensity to give a corrected NAD(P)H trace. When NAD(P)H was measured separately from $[Ca^{2+}]_c$, the 360 nm fluorescence signal was corrected only for photobleaching. To measure $[Ca^{2+}]_c$ and $[Ca^{2+}]_m$ simultaneously, hepatocytes were co-loaded with fura-2 AM and dihydrorhod-2 AM as described in Hajnóczky *et al*. (1995). Fura-2 and rhod-2 fluorescence images were acquired by alternating excitation at 380 nm (fura-2) and 548 nm (rhod-2). The emitted fluorescence was collected using a fura-2/rhodamine dichroic beamsplitter and emission filter set (Chroma Technology).

Imaging measurements of $[Ca^{2+}]_c$ and ΔpH_m or $\Delta\Psi_m$

For simultaneous measurement of $[Ca^{2+}]_c$ and ΔpH_m, hepatocytes were loaded with fura-2 AM and 50 nM fluorescein diacetate for 30–40 min. Fura-2 and fluorescein fluorescence images were acquired by alternating excitation at 340, 380 and 495 nm using a computer-controlled filter wheel and shutter. The emitted fluorescence was collected using a fura-2/BCECF dichroic beamsplitter and a 515 nm long band pass emission filter (Chroma Technology). Fluorescein fluorescence contaminates the fura-2 fluorescence intensity signal to a small extent, so conversion of the fura-2 ratio into $[Ca^{2+}]_c$ was not possible. When $[Ca^{2+}]_c$ and $\Delta\Psi_m$ were measured simultaneously, fura-2-loaded hepatocytes were pre-incubated for 60 min in a KR-HEPES buffer containing 5 nM TMREE prior to transferring both coverslip and TMREE-containing buffer to the microscope chamber. This pre-incubation was necessary to allow TMREE to reach equilibrium across the mitochondrial membrane. In the presence of BSP, no significant loss of fura-2 fluorescence was noted during the pre-incubation. Fura-2 and TMREE fluorescence images were acquired by alternating excitation at 340, 380 and 548 nm. The emitted fluorescence was collected as described above. Values for $[Ca^{2+}]_c$ were calculated from the 340/380 nm ratio after correction for autofluorescence. Autofluorescence values were obtained at the end of each experiment by permeabilizing the hepatocytes with digitonin (20 μg/ml) in an intracellular-like medium containing Ca^{2+}/EGTA buffer and 2 mM ATP·Mg. The fura-2 calibration parameters were determined *in vitro* using a K_d value of 224 nM. Under these experimental conditions, the fura-2 and TMREE fluorescence intensity signals did not overlap, nor was there any effect of TMREE on the calculated $[Ca^{2+}]_c$ values. The TMREE fluorescence intensity was calibrated at the end of each experiment by the addition of 1 μM nigericin, to hyperpolarize the mitochondrial inner membrane, followed by the uncoupler, 1799, plus oligomycin (5 μg/ml each) to obtain the minimum fluorescence values. Oligomycin was included to block uncoupler-stimulated ATP hydrolysis. The addition of the solvent, dimethylsulfoxide (DMSO), to TMREE-loaded hepatocytes causes a small but significant increase in the 548 nm fluorescence signal in the absence of any $[Ca^{2+}]_c$ changes. The subsequent addition of Ca^{2+}-mobilizing agents results in a larger increase in 548 nm fluorescence on top of that observed with DMSO alone (data not shown). The addition of DMSO to fluorescein-loaded hepatocytes had no effect on 495 nm fluorescence intensity (data not shown). Thus, it appears that DMSO has a non-specific effect on TMREE fluorescence which is unrelated to $\Delta\Psi_m$.

Laser scanning confocal microscopy

For simultaneous measurement of MTG (Molecular Probes) and rhod-2 fluorescence, overnight-cultured hepatocytes were incubated with 200 nM MTG for 60 min in WEM plus 10% serum supplemented with 0.005% pluronic acid F-127. The cells were washed and then loaded for 10 min with rhod-2 AM (10 μM) at room temperature in a KR-HEPES buffer plus 0.01% pluronic acid F-127. After loading, the cells were washed extensively with KR-HEPES containing pluronic acid to remove the AM dye prior to switching to a buffer without pluronic acid. Confocal images were acquired using a Bio-Rad MRC 600 laser scanning confocal microscope equipped with a 25 mW argon ion laser. The two dyes were excited simultaneously using the 514 nm laser line, and the emitted red and green fluorescence was collected by separate photomultiplier tubes using the Bio-Rad MRC 600 software and filter sets. The optical section was <1 μm thick.

High resolution measurements of ΔpH_m were performed in overnight-cultured hepatocytes. Hepatocytes were loaded with 200 nM fluorescein diacetate for 40 min in KR-HEPES buffer at room temperature and then washed for 30 min. Confocal images of fluorescein-loaded hepatocytes were acquired with 488 nm excitation and a 515 nm long band pass emission filter. Since fluorescein was very sensitive to bleaching, the laser excitation light was attenuated to $<0.5\%$ transmission. Mitochondrial membrane potential was measured in overnight-cultured hepatocytes pre-incubated for 60–90 min at room temperature in a KR-HEPES buffer containing 5 nM TMREE. Confocal images of TMREE-loaded

hepatocytes were acquired using 514 nm excitation and a 600 nm long band pass emission filter. Laser intensity was attenuated to 1% transmission.

Plasmid construction

cDNAs encoding the N-terminus of cytochrome *c* oxidase (subunit VIII), an HA epitope tag and aequorin (Rutter *et al.*, 1996) were subcloned in-frame into the cytomegalovirus (CMV) immediate early promoter-based expression vector VR1012 (Vical, San Diego, CA; plasmid pCMV*Aq_m). A plasmid encoding untargeted aequorin (pCMV*Aq_c) was constructed by omitting cytochrome *c* oxidase cDNA. Plasmid DNA was purified on two consecutive CsCl gradients, as described by Sambrook *et al.* (1989).

Transfection of hepatocytes

Primary rat hepatocytes were isolated as described above and resuspended at 1.0×10^6 cells/ml in Dulbecco's modified Eagle's medium (DMEM) supplemented with 10% FCS and antibiotics as described by Rutter *et al*. (1996a) for distribution onto poly-D-lysine-coated glass coverslips (13 mm diameter). After culture for 3 h at 37°C, the medium was aspirated carefully and replaced with 1 ml of serum-free medium containing 1 μg of DNA and 2.5 μl of Tfx-50™ (Promega) as per the manufacturer's instructions. After a further 2 h incubation, an additional 1 ml of medium containing 10% serum, was added, and the cells incubated for 24–48 h at 37°C. This method of transfection provided ~1.0% efficiency, as assessed by immunostaining for the transfected aequorin chimera (see below).

Assay of aequorin luminescence and calibration of signals

Expressed aequorin was reconstituted to form the active holoenzyme by incubating transfected hepatocytes for 2 h in serum-free DMEM supplemented with 5 μM coelenterazine (Molecular Probes). Luminescence from cell populations was measured using a low noise photomultiplier (PM) system, with the cells placed in a thermostatted chamber (37°C) maintained 3 mm from the PM tube window (Rutter *et al*., 1993). Cells were superfused constantly (2.5 ml/min) with BSA-free KR-HEPES buffer (see above), and stimuli added by rapidly switching the superfusion medium. At the end of each run, total aequorin was determined by hypotonic cell lysis in the presence of 10 mM $CaCl_2$, 0.1 mg/ml digitonin (Rutter *et al*., 1993). Collected data (1 data point/s) were stored and analyzed off-line using EXCEL™ (Microsoft) to obtain free $[Ca^{2+}]$ from a look-up table as described previously (Rutter *et al*., 1993; Brini *et al*., 1995)

Immunocytochemistry

Transfected cells were fixed with paraformaldehyde and probed with a monoclonal antibody (12CA6) to the HA tag as described by Brini *et al*. (1994). Immunolabeling was revealed with a tetramethylrhodamine isothiocyanate-labeled anti-mouse IgG antibody. Confocal images were obtained using a laser scanning confocal microscope (Leica DM RBE), fitted with a 63×1.3 NA oil-immersion objective with excitation using the 568 nm laser line. Image reconstitution was performed using Imaris™ software on a Silicon Graphics workstation.

Measurement of pyruvate dehydrogenase activity

Hepatocytes plated on Petri dishes were maintained in primary culture for 90 min. The cells were washed twice in KR-HEPES buffer without BSA and once with BSA-containing media. Washed hepatocytes were pre-incubated for 45 min in KR-HEPES buffer at 34°C. This temperature is the approximate buffer temperature in our thermostatically regulated microscope chamber set to 37°C. The buffer was aspirated quickly, and 3 ml of warmed buffer containing the required additions was gently pipetted onto the cells. Incubations were terminated by aspirating the buffer and quickly immersing the Petri dishes into liquid N_2. Ice-cold extraction buffer [100 mM KH_2PO_4, 1 mM Na-EDTA, 5% (v/v) fetal calf serum, 1 mM dithiothreitol, 0.1% Triton X-100, 1 μg/ml of the proteinase inhibitors pepstatin A, antipain and leupeptin, pH 7.3; 150 μl] was then added to the Petri dish on ice, and the cells extracted by scraping. The extracted material was frozen and thawed twice more, to ensure complete disruption of mitochondria, and clarified by centrifugation (10 000 *g*, 1 min, 4°C) before the assay of initial and total PDH activity as described previously (McCormack, 1985; Rutter *et al*., 1996b).

Determination of cellular ATP levels

Hepatocytes were prepared, plated and incubated according the method described above for the determination of PDH activity. After experimental manipulation, cells were extracted with ice-cold perchloric acid (10% v/v, 200 μl), rapidly frozen and stored at –80°C. Determination of ATP was based on published procedures (Stanley and Williams, 1969; Owen and Halestrap, 1993). Briefly, samples were thawed and adjusted to pH 7.4 with a known volume of neutralization mixture (0.5 M triethanolamine, 2 M KOH, 100 mM EDTA). Potassium perchlorate precipitate was removed by centrifugation (10 000 *g*, 2 min) and the supernatant stored on ice prior to assay. Neutralized sample (10 μl) was added to 1 ml of assay buffer (130 mM $NaHAsO_4$, 17 mM $MgSO_4$, 4 mM NaH_2PO_4, pH 7.4) and the reaction was initiated with 10 μg of firefly lantern extract (Sigma, Poole, UK). Emitted light was recorded for 30 s using a photon counting luminometer (LB-9501; EG & Berthold, Bad Wildbad, Germany). Values for cellular ATP (pmoles) were obtained by comparison with known ATP standards (0–20 pmol) prepared in parallel. Protein content was determined in a parallel cell culture by Bradford assay (Bradford, 1976)

Statistical analysis

Data are given as means ± SEM for the number of separate hepatocyte cultures shown in parentheses. Unless otherwise stated in text, all experiments were repeated with at least three separate hepatocyte preparations.

Acknowledgements

We thank Professor A.P.Halestrap (University of Bristol) for helpful advice, Rebecca Schnabel for assistance with immunocytochemistry and Dr John A.Thomas (University of South Dakota) for the inspiration to measure mitochondrial PMF and $[Ca^{2+}]_c$ simultaneously. This work was supported by grants from NIH (DK38422), the Medical Research Council (UK), Nova-Nordisk (Denmark), The British Diabetic Association, The Wellcome Trust, the Royal Society and the Christabel Wheeler bequest. P.B. held a BBSRC CASE postgraduate studentship.

References

Avi-Dor,Y., Olson,J.M., Doherty,M.D. and Kaplan,N.O. (1962) Fluorescence of pyridine nucleotides in mitochondria. *J. Biol. Chem.*, **237**, 2377–2383.

Babcock,D.F., Herrington,J., Goodwin,P.C., Park,Y.B. and Hille,B. (1997) Mitochondrial participation in the intracellular Ca^{2+} network. *J. Cell Biol.*, **136**, 833–844.

Balaban,R.S. and Blum,J.J. (1982) Hormone-induced changes in NADH fluorescence and O_2 consumption of rat hepatocytes. *Am. J. Physiol.*, **242**, C172–C177.

Bradford,M.M. (1976) A rapid and sensitive method for the quantitation of microgram quantities of protein utilizing the principle of protein–dye binding. *Anal. Biochem.*, **72**, 248–254.

Brini,M., Marsault,R., Bastianutto,C., Pozzan,T. and Rizzuto,R. (1994) Nuclear targeting of aequorin. A new approach for measuring Ca^{2+} concentration in intact cells. *Cell Calcium*, **16**, 259–268.

Brini,M., Marsault,R., Bastianutto,C., Alverez,J., Pozzan,T. and Rizzuto,R. (1995) Transfected aequorin in the measurement of cytosolic Ca^{2+} concentration ($[Ca^{2+}]$). A critical evaluation. *J. Biol. Chem.*, **270**, 9896–9903.

Brown,G.C., Lakin-Thomas,P.L. and Brand,M.D. (1990) Control of respiration and oxidative phosphorylation in isolated rat liver cells. *Eur. J. Biochem.*, **192**, 355–362.

Budd,S.L. and Nicholls,D.G. (1996) A reevaluation of the role of mitochondria in neuronal Ca^{2+} homeostasis. *J. Neurochem.*, **66**, 403–411.

Chiavaroli,C., Bird,G.S.J. and Putney,J.W.,Jr (1994) Delayed 'all-or-none' activation of inositol 1,4,5-trisphosphate-dependent calcium signaling in single rat hepatocytes. *J. Biol. Chem.*, **269**, 25570–25575.

Davidson,A.M. and Halestrap,A.P. (1987) Liver mitochondrial pyrophosphate concentration is increased by Ca^{2+} and regulates the intramitochondrial volume and adenine nucleotide content. *Biochem. J.*, **246**, 715–723.

Denton,R.M. and McCormack,J.G. (1980) On the role of the calcium transport cycle in the heart and other mammalian mitochondria. *FEBS Lett.*, **119**, 1–8.

Denton,R.M., Randle,P.J. and Martin,B.R. (1972) Stimulation by Ca^{2+} ions of pyruvate dehydrogenase phosphate phosphatase. *Biochem. J.*, **128**, 161–163.

Denton,R.M., Richards,D.A. and Chin,J.G. (1978) Calcium ions and the regulation of NAD^+-linked isocitrate dehydrogenase of rat heart and other tissues. *Biochem. J.*, **176**, 899–906.

Denton,R.M., McCormack,J.G., Rutter,G.A., Burnett,P., Edgell,N.J., Moule,S.K. and Diggle,T.A. (1996) Hormonal regulation of the pyruvate dehydrogenase complex. *Adv. Enzyme Regul.*, **36**, 183–198.

Duchen,M.R. (1992) Ca^{2+}-dependent changes in the mitochondrial energetics in single dissociated mouse sensory neurons. *Biochem. J.*, **283**, 41–50.

Gunter,T.E., Gunter,K.K., Sheu,S.S. and Gavin,C.E. (1994) Mitochondrial calcium transport: physiological and pathological relevance. *Am. J. Physiol.*, **267**, C313–C339.

Hajnóczky,G., Robb-Gaspers,L.D., Seitz,M.B. and Thomas,A.P. (1995) Decoding of cytosolic calcium oscillations in the mitochondria. *Cell*, **82**, 415–424.

Halestrap,A.P. (1989) The regulation of the matrix volume of mammalian mitochondria *in vivo* and *in vitro* and its role in the control of mitochondrial metabolism. *Biochim. Biophys. Acta*, **973**, 355–382.

Halestrap,A.P. and Dunlop,J.L. (1986) Intramitochondrial regulation of fatty acid β-oxidation occurs between flavoprotein and ubiquinone. *Biochem. J.*, **239**, 559–565.

Hansford,R.G. (1994) Physiological role of mitochondrial Ca^{2+} transport. *J. Bioenerg. Biomembr.*, **26**, 495–508.

Hems,D.A., McCormack,J.G. and Denton,R.M. (1978) Activation of pyruvate dehydrogenase by vasopressin. *Biochem. J.*, **176**, 627–629.

Hoek,J.B. (1992) Hormonal regulation of cellular energy metabolism. In Ernster,L. (ed.), *Molecular Mechanisms in Bioenergetics*. Elsevier Science Publishers B.V., Amsterdam, The Netherlands, pp. 421–461.

Hoek,J.B., Nicholls,D.G. and Williamson,J.R. (1980) Determination of the mitochondrial proton motive force in isolated hepatocytes. *J. Biol. Chem.*, **255**, 1458—1464.

Hoth,M., Fanger,C.M. and Lewis,R.S. (1997) Mitochondrial regulation of store-operated calcium signaling in T lymphocytes. *J. Cell Biol.*, **137**, 633–648.

Jouaville,L.S., Ichas,F., Holmuhamedov,E.L., Camacho,P. and Lechleiter,J.D. (1995) Synchronization of calcium waves by mitochondrial substrates in *Xenopus laevis* oocytes. *Nature*, **377**, 438–441.

Loew,L.M., Tuft,R.A., Carrington,W. and Fay,F.S. (1993) Imaging in five dimensions: time-dependent membrane potentials in individual mitochondria. *Biophys. J.*, **65**, 2396–2407.

Loew,L.M., Carrington,W., Tuft,R.A. and Fay,F.S. (1994) Physiological cytosolic Ca^{2+} transients evoke concurrent mitochondrial depolarizations. *Proc. Natl Acad. Sci. USA*, **91**, 12579–12583.

McCormack,J.G. (1985) Studies on the activation of rat liver pyruvate dehydrogenase and 2-oxoglutarate dehydrogenase by adrenaline and glucagon. Role of increases in intramitochondrial Ca^{2+} concentration. *Biochem. J.*, **231**, 597–608.

McCormack,J.G. and Denton,R.M. (1979) The effects of calcium ions and adenine nucleotides on the activity of pig heart 2-oxoglutarate dehydrogenase complex. *Biochem. J.*, **180**, 533–544.

McCormack,J.G., Halestrap,A.P. and Denton,R.M. (1990) Role of calcium ions in regulation of mammalian intramitochondrial metabolism. *Physiol. Rev.*, **70**, 391–425.

Nicholls,D.G. (1978) The regulation of extramitochondrial free calcium ion concentration by rat liver mitochondria. *Biochem. J.*, **176**, 463–474.

Oviasu,O.A. and Whitton,P.D. (1984) Hormonal control of pyruvate dehydrogenase activity in rat liver. *Biochem. J.*, **224**, 181–186.

Owen,M.R. and Halestrap,A.P. (1993) The mechanisms by which mild respiratory chain inhibitors inhibit hepatic gluconeogenesis. *Biochim. Biophys. Acta*, **1142**, 11–22.

Pralong,W.F., Spat,A. and Wollheim,C.B. (1994) Dynamic pacing of cell metabolism by intercellular Ca^{2+} transients. *J. Biol. Chem.*, **269**, 27310–27314.

Prpic,V., Spencer,T.L. and Bygrave,F.L. (1978) Stable enhancement of calcium retention in mitochondria isolated from rat liver after the administration of glucagon to the intact animal. *Biochem. J.*, **176**, 705–714.

Quinlan,P.T. and Halestrap,A.P. (1986) The mechanism of the hormonal activation of respiration in isolated hepatocytes and its importance in the regulation of gluconeogenesis. *Biochem. J.*, **236**, 789–800.

Reed,L.J. and Yeaman,S.J. (1987) Pyruvate dehydrogenase. In Boyer,P.D. and Krebs,E.G. (eds), *The Enzymes*. Academic Press, New York, pp. 77–93.

Rizzuto,R., Brini,M., Murgia,M. and Pozzan,T. (1993) Microdomains with high Ca^{2+} close to IP_3-sensitive channels that are sensed by neighboring mitochondria. *Science*, **262**, 744–747.

Rizzuto,R., Bastianutto,C., Brini,M., Murgia,M. and Pozzan,T. (1994) Mitochondrial Ca^{2+} homeostasis in intact cells. *J. Cell Biol.*, **126**, 1183–1194.

Robb-Gaspers,L.D. and Thomas,A.P. (1995) Coordination of Ca^{2+} signaling by intercellular propagation of Ca^{2+} waves in the intact liver. *J. Biol. Chem.*, **270**, 8102–8107.

Rooney,T.A., Sass,E.J. and Thomas,A.P. (1989) Characterization of cytosolic calcium oscillations induced by phenylephrine and vasopressin in single fura-2-loaded hepatocytes. *J. Biol. Chem.*, **264**, 17131–17141.

Rutter,G.A. (1990) Ca^{2+}-binding to citrate cycle enzymes. *Int. J. Biochem.*, **22**, 1081–1088.

Rutter,G.A., Theler,J.-M., Murta,M., Wollheim,C.B., Pozzan,T. and Rizzuto,R. (1993) Stimulated Ca^{2+} influx raises mitochondrial free Ca^{2+} to supramicromolar levels in a pancreatic β-cell line: possible role in glucose and agonist-induced insulin secretion. *J. Biol. Chem.*, **268**, 22385–22390.

Rutter,G.A., Burnett,P., Brini,M., Pozzan,T., Tavare,J.M., Denton,R.M. and Rizzuto,R. (1996a) Imaging intramitochondrial Ca^{2+} with recombinant targeted aequorin. *J. Physiol.*, **493P**, 16–17.

Rutter,G.A., Burnett,P., Rizzuto,R., Brini,M., Murgia,M., Pozzan,T., Tavare,J.M. and Denton,R.M. (1996b) Subcellular imaging of intramitochondrial Ca^{2+} with recombinant targeted aequorin: significance for the regulation of pyruvate dehydrogenase activity. *Proc. Natl Acad. Sci. USA*, **93**, 5489–5494.

Sambrook,J., Fritsch,E.F. and Maniatis,T. (1989) *Molecular Cloning: A Laboratory Manual*. Cold Spring Harbor Laboratory Press, Cold Spring Harbor, NY.

Simpson,P.B.and Russell,J.T. (1996) Mitochondria support inositol 1,4,5-trisphosphate-mediated Ca^{2+} waves in cultured oligodendrocytes. *J. Biol. Chem.*, **271**, 33493–33501.

Soboll,S. (1993) Long-term and short-term changes in mitochondrial parameters by thyroid hormones. *Biochem. Soc. Trans.*, **21**, 799–803.

Soboll,S. and Scholz,R. (1986) Control of energy metabolism by glucagon and adrenaline in perfused rat liver. *FEBS Lett.*, **205**, 109–112.

Soboll,S., Horst,C., Hummerich,H., Schumacher,J.P. and Seitz, H.J. (1992) Mitochondrial metabolism in different thyroid states. *Biochem. J.*, **281**, 171–173.

Stanley,P.E. and Williams,S.G. (1969) Use of the liquid scintillation spectrometer for determining adenosine triphosphate by the luciferase enzyme. *Anal. Biochem.*, **29**, 381–392.

Strzelecki,T., Strzelecka,D., Koch,C.D. and LaNoue,K.F. (1988) Sites of action of glucagon and other Ca^{2+} mobilizing hormones on the malate aspartate cycle. *Arch. Biochem. Biophys.*, **264**, 310–320.

Sugano,T., Shiota,M., Khono,H., Shimada,M. and Oshino,N. (1980) Effects of calcium ions on the activation of gluconeogenesis by norepinephrine in perfused rat liver. *J. Biochem.*, **87**, 465–472.

Sugano,T., Nishimura,K., Sogabe,N., Shiota,M., Oyama,N., Noda,S. and Ohta,M. (1988) Ca^{2+}-dependent activation of the malate-aspartate shuttle by norepinephrine and vasopressin in perfused rat liver. *Arch. Biochem. Biophys.*, **264**, 144–154.

Taylor,W.M., Prpic,V., Exton,J.H. and Bygrave,F.L. (1980) Stable changes to calcium fluxes in mitochondria isolated from rat livers perfused with α-adrenergic agonists and with glucagon. *Biochem. J.*, **188**, 443–450.

Thomas,P.J., Gaspers,L.D., Pharr,C. and Thomas,J.A. (1991) Continuous measurement of mitochondrial pH gradients in isolated hepatocytes by difference ratio spectroscopy. *Arch. Biochem. Biophys.*, **288**, 250–261.

Whitehouse,S., Cooper,R.H. and Randle,P.J. (1974) Mechanism of activation of pyruvate dehydrogenase by dichloroacetate and other halogenated carboxylic acids. *Biochem. J.*, **141**, 761–774.

Received January 22, 1998; revised July 3, 1998; accepted July 6, 1998